# Neural instructive signals for associative cerebellar learning

N. Tatiana Silva[1], Jorge Ramírez-Buriticá[1], Dominique L. Pritchett[1,2,*] and Megan R. Carey[1,*]

[1]*Neuroscience Program, Champalimaud Center for the Unknown, Lisbon Portugal*
[2]*Biology Dept., Howard University, Washington D.C.*

*Correspondence:
megan.carey@neuro.fchampalimaud.org
dominique.pritchett@howard.edu

**AUTHOR CONTRIBUTIONS**

NTS designed the research plan, performed all experiments and data analysis, prepared figures, and wrote the manuscript. JRB performed and analyzed electrophysiological recordings. DLP designed the research plan, performed experiments and analysis, and provided supervision. MRC designed the research plan, provided supervision, and wrote the manuscript.

**COMPETING INTERESTS**

The authors declare no competing financial interests**.**

**ABSTRACT**

Supervised learning depends on instructive signals that shape the output of neural circuits to support learned changes in behavior. Climbing fiber inputs to the cerebellar cortex represent one of the strongest candidates in the vertebrate brain for conveying neural instructive signals. However, recent studies have shown that Purkinje cell stimulation can also drive cerebellar learning, and the relative importance of these two neuron types in providing instructive signals for cerebellum-dependent behaviors remains unresolved. Here we used cell-type specific perturbations of climbing fibers, Purkinje cells, and other cerebellar circuit elements to systematically evaluate their contributions to delay eyeblink conditioning. Our findings reveal that while optogenetic stimulation of either climbing fibers or Purkinje cells can substitute for a sensory unconditioned stimulus, subtle reductions in climbing fiber signaling prevent learning entirely. We conclude that climbing fibers and corresponding Purkinje cell complex-spike events provide essential instructive signals for associative cerebellar learning.

## INTRODUCTION

Instructive signals are a core component of supervised learning systems. In the brain they are thought to be conveyed by specific classes of neurons that trigger modification of neural pathways that control behavior. Climbing fiber projections from the inferior olive to the cerebellar cortex have long-been hypothesized to convey neural instructive error signals for various forms of learning, including associative eyeblink conditioning and several forms of motor adaptation[1–8].

According to the climbing fiber hypothesis, climbing fiber activity drives heterosynaptic plasticity at parallel fiber inputs to cerebellar Purkinje cells, which forms the neural substrate for learning. There are several lines of evidence in support of this hypothesis. Climbing fibers evoke powerful complex spikes in cerebellar Purkinje cells, elevating postsynaptic calcium and driving associative synaptic plasticity at parallel fiber-to-Purkinje cell synapses[9–12]. Complex spike activity is associated with sensorimotor errors for a range of behavioral tasks, with the probability of a complex spike often changing in predictable ways with the development of learning[13–20], and its extinction[21–23]. Moreover, electrical stimulation of climbing fiber pathways is sufficient to substitute for an air-puff unconditioned stimulus to drive eyeblink conditioning in rabbits[24,25], and recent experiments have shown that optogenetic climbing fiber stimulation can trigger adaptation of the vestibulo-ocular reflex[26,27], while inhibition of CFs can drive extinction of eyeblink conditioning[22,23].

However, significant controversy remains, particularly regarding the necessity of climbing fiber  instructive signals and complex spike-driven plasticity for learning[7,28–33]. Much of the evidence to date for the necessity of climbing fiber instructive signals for cerebellar learning has come from lesion studies[34], pharmacological inactivations[22,28], and electrical perturbations[35,36] of the inferior olive. These manipulations, which lack both cell-type and temporal specificity, are likely to have substantial additional, unintended effects on the olivocerebellar circuit[37].

There is also substantial experimental support for an alternative model which posits that Purkinje cell simple spike modulation itself could provide relevant instructive signals for learning[4,38]. Sensorimotor errors that drive climbing fiber activity and subsequent Purkinje cell complex spikes often also evoke rapid reflexive, corrective movements. Neural representations of these corrective movements could provide instructive signals for plasticity – either in addition to, or independently of, complex spike activity[29,38–44]. Indeed, Purkinje cell simple spike output often correlates with these corrective movements[32,45,46]. Purkinje cell simple spike modulation could then instruct plasticity in the cerebellar nuclei, an idea that also has support from in vitro experiments of synaptic plasticity[47,48].

Consistent with a possible role for Purkinje cell instructive signals in cerebellar learning, repeated optogenetic stimulation of Purkinje cells paired with ongoing movements has been recently shown to drive movement adaptation in multiple systems[26,49,50]. However, it is not clear whether this optogenetically-evoked learning results from modulation of simple spike output that instructs plasticity in the cerebellar nuclei (as originally hypothesized by Miles & Lisberger, 1981), or rather, from optogenetically-evoked complex spike-like events in Purkinje cell dendrites that instruct plasticity in the cerebellar cortex[50]. Thus, these experiments alone cannot distinguish between simple spike output or dendritic calcium signaling in Purkinje cells as providing the effective instructive signals for learning.

Here we used cell-type specific perturbations of climbing fibers, Purkinje cells, and other circuit elements to test their necessity and sufficiency for associative cerebellar learning. We combined behavioral, optogenetic and electrophysiological approaches to dissociate climbing fiber inputs and complex spike activity from reflexive movements and simple spike modulation. We find that optogenetically-evoked complex spikes can substitute for an air-puff unconditioned stimulus to induce learning, even in the absence of an evoked blink. Direct optogenetic stimulation of Purkinje cells can also drive learning; however, this effect was dissociable from both simple spike modulation and the corresponding evoked blink. Finally, simple ChR2 expression in climbing fibers is associated with a subtle decrease in Purkinje cell complex-spike probability that abolishes learning to a sensory unconditioned stimulus. Together, our results support a necessary and sufficient role for climbing fibers and corresponding Purkinje cell complex spike-events as instructive signals for associative cerebellar learning.

**RESULTS**

We investigated neural instructive signals for delay eyeblink conditioning in head-fixed mice walking on a motorized treadmill[51,52]. In classical eyeblink conditioning experiments (Fig. 1a), a neutral conditioned stimulus (CS, here a white light LED) is paired with an unconditioned stimulus (US, usually a puff of air directed at the eye) that reliably elicits an eyeblink unconditioned response (UR) and serves as an instructive signal for learning. We first asked whether direct optogenetic stimulation of climbing fibers could substitute for a sensory (air-puff) US to drive behavioral learning (Fig. 1a).

**Optogenetic climbing fiber stimulation is sufficient to drive eyeblink conditioning**
To specifically target climbing fibers (CF), we injected a virus that allows for expression of ChR2 under control of the CaMKIIα promoter[26] (AAV-CaMKII-ChR2) into the inferior olive (IO) of wildtype mice (Fig. 1a,b; Methods; Supp. Table 1). With this strategy we observed selective labeling of neurons in the IO and climbing fibers in the cerebellar cortex (Fig. 1c; Supp. Fig. 1). An optical fiber was placed either in the eyelid region of the cerebellar cortex[53–56], targeting CF terminals (CF-ChR2-Ctx), or the dorsal accessory IO[23,24,26] (CF-ChR2-IO), targeting cell bodies of eyeblink-related climbing fibers (Fig. 1b; Supp. Fig. 1; Methods). Laser stimulation at both sites evoked robust postsynaptic complex spike responses in cerebellar Purkinje cells, although with slightly different dynamics depending on the stimulation site (Fig. 1d-g), with waveforms matching those of spontaneous complex spikes (Fig. 1h).

To test the sufficiency of climbing fiber activity for acquisition of learned eyelid responses, we paired a neutral visual CS with optogenetic CF stimulation in the absence of any sensory US (CF-ChR2-US; Fig. 1a). Laser stimulation alone did not elicit eyelid closures in these mice (Supp. Fig. 1g). Despite the absence of an eyeblink unconditioned response (UR) to the optogenetic-US, conditioned eyelid closure responses (CRs) gradually emerged in response to the visual CS following repeated CS+US pairing (Fig. 1i-l). Similar learning was observed for fiber placements in either the IO (CF-ChR2-IO; Fig. 1i,j) or the cerebellar cortex (CF-ChR2-Ctx; Fig. 1k,l; though note the subtly different CR timings in the two cases; Supp. Fig. 1j,k). Moreover, learning was also observed in separate experiments in which we targeted ChR2 expression to glutamatergic IO neurons with a transgenic, rather than viral strategy, by crossing VGlut2-Cre mice with ChR2-floxed mice[57] (*Vglut2-Cre;ChR2*; Supp. Table 1*)* and placing the fiber in the IO (VGlut2-ChR2-IO; Supp. Fig. 1l-o).

In general, the properties of learning to an optogenetic CF-US matched those of normal sensory CS+US conditioning in wildtype mice[51,52]. Learning to an optogenetic-US emerged over several days, with the amplitudes of learned eyelid closures, measured on CS-only trials, increasing gradually across sessions (Fig. 1i-l). Learning also extinguished appropriately upon cessation of CS+US pairing, when CS's were presented alone (Supp. Fig. 1h). Moreover, responses were unilateral (Supp. Fig. 1i) and their peaks were appropriately timed to correspond to the arrival of the US (Fig. 1j,l).

A central feature of eyeblink conditioning is the appropriate timing of the CR, so that its peak generally coincides with the expected time of the arrival of the US[58,59]. We therefore tested whether learning to an optogenetic-US could also be adapted for varying CS+US interstimulus intervals. Indeed, when the interval between CS and CF-ChR2-US onset was

shifted from 300ms to 500ms, mice adapted the timing of their learned responses[52,59] (Fig. 1m).

These results indicate that optogenetic climbing fiber activation is sufficient to substitute for an air-puff US to instruct delay eyeblink conditioning.

**Optogenetic stimulation of Purkinje cells can substitute for a US to drive learning**
Optogenetic stimulation of Purkinje cells has previously been shown to instruct motor adaptation of limb and eye movements[26,49,50]. To investigate whether this was also true for delay eyeblink conditioning, we placed an optical fiber at the eyelid region of the cerebellar cortex of transgenic mice expressing ChR2 under the L7 Purkinje-cell specific promoter (*L7-Cre;Chr2* mice; Fig. 2a,b; Supp. Table 1). In vivo electrophysiological recordings confirmed an increase in Purkinje cell simple spike activity at the onset of stimulation, followed by a decrease below the baseline firing rate upon the cessation of stimulation (Fig. 2c,d).

Eyelid closures are associated with decreases in Purkinje cell simple spike firing rate in the eyelid region of cerebellar cortex[54–56,60]. Consistent with this, and with previous optogenetic studies[51,54], we found that optogenetic Purkinje cell stimulation with low-medium laser intensities resulted in an eyelid closure upon stimulus offset whose amplitude scaled as a function of laser intensity (Fig. 2e).

When a visual CS was consistently paired with optogenetic stimulation of Purkinje cells that led to a blink at laser offset as a US (Pkj-ChR2-Ctx; Fig. 2f), robust conditioned responses gradually emerged (Fig. 2g,h). Rates of learning and conditioned response amplitudes were comparable to those obtained with an air-puff US [51], and also with the CF-ChR2-US used in Fig. 1.

The results of Fig. 2 suggest that direct optogenetic stimulation of Purkinje cells can substitute for an air-puff unconditioned stimulus to drive eyeblink conditioning. However, they do not dissociate between the effects of optogenetic stimulation on Purkinje cell simple spikes, complex spikes, and evoked eyelid closures. In the next set of experiments we altered the temporal relationships between these candidate instructive signals by systematically varying laser timing, duration, and intensity (Supp. Fig. 2).

**Onset of Purkinje cell optogenetic stimulation drives learning independently of simple spike modulation or an evoked blink**
The well-timed conditioned responses observed in eyeblink conditioning are thought to be a consequence of plasticity mechanisms acting within the cerebellar cortex that associate postsynaptic calcium events (usually complex spikes) in Purkinje cells with a particular set of parallel fiber inputs active within a particular temporal window from the onset of the conditioned stimulus[4–6,12,58,61]. We first asked whether learning to an optogenetic Pkj-US would yield well-timed conditioned responses (Fig. 3b). Indeed, extending the interstimulus interval between CS and Pkj-ChR2-US onset from 200ms to 400ms revealed appropriate corresponding shifts in CR timing (Fig. 3c-e).

Having thus established that learned responses to an optogenetic Pkj-US can be appropriately timed, we next varied the duration of laser stimulation (Fig. 3f; Supp. Fig. 2e-g) to determine whether conditioned responses were timed to match the onset of Pkj-ChR2-stimulation or its offset and the associated blink. To do this we compared conditions

6

in which the onset of Purkinje cell stimulation was presented at the same interstimulus interval relative to the CS, but the offset (and its respective complex spike and blink) differed by 200ms (Fig. 3f,g; Supp. Fig. 2e-g). The conditioned response amplitudes and timings were identical in the two groups (Fig. 3h,i). This result suggests that events associated with the *onset* of optogenetic stimulation, and not the abrupt decrease in simple spike rate or the corresponding blink evoked at laser offset, are crucial for learning driven by optogenetic stimulation of Purkinje cells.

We next exploited the relationship between laser power, simple spike modulation, and timing of the evoked blink to further disambiguate which consequences of optogenetic stimulation were responsible for optogenetically-driven learning. At higher powers, laser stimulation induces a pause in Purkinje cell simple spike activity at laser onset (Supp. Fig. 2h,i), likely due to depolarization block[62,63]. Consistent with this and the well-established relationship between Purkinje cell simple spike inhibition and eyelid closures, we found that increasing laser intensity also led to a temporal shift in the timing of the optogenetically-evoked blink – from laser offset, to laser onset (Fig. 3j,k; Supp. Fig. 2j). We took advantage of this feature to compare learning under conditions in which the timing and duration of the optogenetic 'US' stimulation were identical, but laser power was adjusted to invert the direction of simple spike modulation and shift the timing of the evoked blink from laser offset to laser onset (Fig. 3j,k; Supp. Fig. 2h-j). As in the experiment presented in Fig. 3f-i, here, too, we found that conditioned response timing depended only on the timing of laser onset, and not the timing of the evoked blink on the paired trials (Fig. 3l,m). This again suggests that the relevant instructive signal for learning occurs at the onset, and not offset, of Purkinje cell optogenetic stimulation. Moreover, because of the switch from laser onset-induced increases in simple spike activity to laser onset-evoked pauses in simple spike activity at high intensities (Supp. Fig. 2h,i), it further dissociates laser onset from the modulation of Purkinje cell simple spike output as the relevant instructive stimulus for learning.

Taken together, the results of Figs. 2 and 3 suggest that while Purkinje cell optogenetic stimulation can substitute for an air-puff US to drive eyeblink conditioning, the effective instructive stimulus driving this learning is tightly linked to the onset of laser stimulation but independent of simple spike modulation or the blink that it evokes. One possible explanation for this finding would be if Pkj-ChR2 stimulation triggers complex spike-like events in the form of dendritic calcium signals that are capable of driving learning, as has been recently demonstrated for VOR adaptation[50]. Consistent with this possibility, we observed consistent complex spike-like events at the onset of Pkj-ChR2 stimulation at higher stimulation intensities (Supp. Fig. 2k).

If Pkj-ChR2-US stimulation drives eyeblink learning through the generation of complex spike-like events, then we would predict that Purkinje cell modulation driven by synaptic inputs rather than direct optogenetic stimulation might not be sufficient to induce learning, even if it was strong enough to modulate Purkinje cell simple spikes and evoke a blink. To test this prediction, we replaced direct Pkj-ChR2 stimulation with optogenetic stimulation of cerebellar granule cells, the source of parallel fiber inputs to Purkinje cells (Gabra6-ChR2-Ctx; Fig. 4a,b; Supp. Table 1). As we showed previously, granule cell stimulation drives a blink at laser onset, consistent with net inhibition of Purkinje cells via molecular layer interneurons [51](Fig. 4c). Although this stimulation effectively modulated Purkinje cell simple spikes (Fig. 4d,e) and drove a blink (Fig. 4c,f), it did not generate a complex spike-like-

event (Fig. 4d,e), and pairing it with a visual conditioned stimulus did not result in learning (Fig. 4 f-h).

The most parsimonius interpretation of the data presented in (Figs. 2-4 and Supp. Fig. 2) is that optogenetic stimulation of Purkinje cells drives learning through complex spike-like events associated with stimulation onset[50] (Supp. Fig. 4).

**Optogenetic perturbation of the inferior olive impairs eyeblink conditioning**
We next used several complementary approaches to ask whether climbing fiber activity is *required* for delay eyeblink conditioning to a sensory air-puff US. In the first approach, we optogenetically manipulated IO activity only during the presentation of CS+US trials (Fig. 5). These experiments were modeled on previous work[35] using stimulation-based approaches to perturb IO signaling, presumably by depleting synaptic transmission at the rapidly depressing climbing fiber synapses[64] (Fig. 5a,b). For these experiments we first targeted glutamatergic IO neurons using *Vglut2-Cre;ChR2* transgenic mice with a fiber placed in the dorsal IO[57] (vGlut2-ChR2-IO; Fig. 5a-c; see also Supp. Fig. 1). Sustained optogenetic stimulation throughout each CS+US presentation strongly suppressed learning; animals never reached the same percentage nor amplitude of CR as did all controls (that either expressed ChR2 in the same neurons, without laser stimulation, or had IO laser stimulation without ChR2 expression) (Fig. 5d-f). Next we targeted excitatory inputs to the IO by placing an optic fiber at the dorsal accessory IO of *Thy1-ChR2* mice, in which ChR2 is expressed in glutamatergic inputs to the IO but not within the IO itself[51,65,66] (Thy1-ChR2-IO; Fig. 5g-i). Optogenetic perturbation of these IO inputs also strongly impaired learning to an air-puff US (Fig. 5j-l).

**Subtle reductions in climbing fiber signaling eliminate eyeblink conditioning**
We had initially planned to repeat the experiments shown in Fig. 5 in mice with climbing fiber-specific ChR2 expression (CF-ChR2), taking advantage of the same CaMKII promoter strategy that we had used in Fig. 1. Surprisingly, however, we found that CF-ChR2-expressing animals were unable to learn in traditional eyeblink experiments using a sensory air-puff US, even in the absence of any laser stimulation (Fig. 6a-d). In other words, simply expressing ChR2 in climbing fibers completely blocked normal behavioral learning. This surprising result held true despite the facts that, as we have already shown: 1) ChR2-expression was specific to climbing fibers in these mice (Fig. 1c; Supp. Fig. 1). 2) Spontaneous Purkinje cell complex spikes were generally observed in these animals (Fig. 1d-g,k). 3) Complex spikes were readily evoked by CF-optogenetic stimulation (Fig. 1d-h). 4) The mice displayed intact behavioral unconditioned responses (blinks) to the air-puff (Fig. 6a), indicating intact sensory processing. And of course, CF-ChR2 animals learned well to an optogenetic CF-ChR2-US (Fig. 1i-l).

Although we had used standard parameters for viral ChR2 expression[26,50,67] and there was no obvious indication of ChR2 overexpression, we next asked whether lower levels of ChR2-expression in climbing fibers could restore learning to a sensory US (Fig. 6). We therefore repeated the experiments of Fig. 1 and Fig. 6a-d but now with an extra 5-fold dilution of viral titer (CF-ChR2-LE; 1,31x10^11 vs. 2,62x10^12 GC/ml final concentration; Methods). As with the original viral titer, Purkinje cells in mice with lower ChR2 expression (CF-ChR2-LE) also exhibited laser-evoked complex spikes in response to laser stimulation in IO or Ctx (Supp. Fig. 3; compare with Fig. 1d-g). These animals also learned well when an optogenetic CF-ChR2-US was paired with a conditioned stimulus (Fig. 6f,h; compare

with Fig. 1i,j). Critically, the ability to learn to a sensory air-puff US was also restored in CF-ChR2-LE mice (Fig. 6j-l).

To understand how simply expressing ChR2 at moderate levels in climbing fibers could have such a remarkable and selective impact on learning to a sensory US, we quantitatively compared electrophysiological recordings from Purkinje cells in CF-ChR2, CF-ChR2-LE, and control mice (Fig. 7). We analyzed spontaneous simple and complex spikes as well as responses to an air-puff stimulus delivered to the eye (Fig. 7a-f). In control conditions, complex spikes are relatively infrequent, with a low average spontaneous firing rate, and substantial variation across cells (Fig. 7g). We observed subtly lower spontaneous complex spike rates in Purkinje cells of CF-ChR2 mice compared to controls, while no significant reduction was observed in CF-ChR2-LE mice (Fig. 7g). Remarkably, we also found that some (4/15) units with moderate CF-ChR2 expression that showed clear short-latency complex spikes upon CF-ChR2 stimulation did not exhibit any spontaneous complex spikes throughout the duration of our recordings (Fig. 7g). We note that traditional identification of Purkinje cells using the presence of spontaneous complex spikes would therefore underestimate the overall effect of CF-ChR2 expression on climbing fiber-Purkinje cell transmission.

Beyond the effects on spontaneous complex spikes, we observed a clear reduction in the probability of complex spikes evoked by an air-puff stimulus in CF-ChR2 mice (Fig. 7h). This was true across the population of Purkinje cells we recorded from these mice, including those with normal spontaneous complex spike rates (Fig. 7i). In contrast, no systematic reduction in air-puff evoked complex spiking was observed in CF-ChR2-LE animals (Fig. 7h). Further, on trials in which an air-puff did evoke Purkinje cell complex spikes, the responses were delayed in Purkinje cells recorded from CF-ChR2, but not CF-ChR2-LE mice (Fig. b,d,f,j).

Importantly, none of the differences in complex spiking observed in CF-ChR2 animals were associated with differences in Purkinje cell simple spike statistics, including average SS firing rate, coefficient of variation, or the pause in simple spikes following a complex spike (Fig. 7k-m).

DISCUSSION

The climbing fiber hypothesis for cerebellar learning has dominated the field for over 50 years[1–3], yet definitive proof – or disproof – has remained elusive. While multiple experimental approaches have yielded data consistent with the theory, other studies have provided support for an alternative model, in which Purkinje cell simple spike modulation, rather than complex spikes, provides critical instructive signals for learning[4,29,38,43]. Moreover, while sensorimotor errors that drive behavioral learning are often reflected in climbing fiber-driven Purkinje cell CSpk activity, the correlational nature of most of these studies, combined with the unusual spiking statistics of complex spikes, have complicated a definitive interpretation of CSpks as instructive signals[32]. Here we systematically manipulated distinct circuit elements to dissociate climbing fiber signaling from Purkinje cell simple spike modulation and reflexive movements. Our findings reveal climbing fiber inputs as essential instructive signals for associative cerebellar learning.

All of the results presented here point to a critical role for complex-spike like events in Purkinje cells – driven either by climbing fiber synaptic inputs or by direct Purkinje cell optogenetic stimulation – in providing instructive signals for delay eyeblink conditioning (Supp. Fig. 4). As has been recently shown for VOR adaptation[26,27,50], we found that optogenetic stimulation of both climbing fibers and Purkinje cells can substitute for a sensory US to drive eyeblink conditioning (Figs. 1-2, Supp. Fig. 1). In both cases, learning was independent of an evoked blink (Figs. 1-3, Supp. Figs. 1-2). However, experiments varying opto-Pkj-US laser intensity and duration revealed that learning to a Purkinje cell optogenetic US was temporally coupled to optogenetic US onset, regardless of the direction of Purkinje cell simple spike modulation, or the timing of an evoked blink (Fig. 3). Further experiments in which Purkinje cell simple spike modulation was achieved indirectly, through optogenetic stimulation of granule cells, also failed to induce learning (Fig. 4). Taken together (Supp. Fig. 4), these findings suggest that optogenetic stimulation of Purkinje cells likely drives learning through the generation of complex spike-like dendritic calcium signals (Supp. Fig. 2H), which have been recently demonstrated for VOR adaptation[50], rather than through modulation of simple spike output.

Beyond demonstrating their sufficiency as instructive signals for learning, multiple aspects of our data point to the necessity of intact climbing fiber signaling for delay eyeblink conditioning (Supp. Fig. 4). One line of evidence came from experiments in which selective optogenetic perturbation of either glutamatergic IO neurons or excitatory inputs to the IO during CS+US trials impaired eyeblink conditioning to an air-puff US (Fig. 5). But the strongest evidence came from our surprising finding that simply expressing ChR2 in climbing fibers – in the absence of any optical stimulation – reduced complex spike probability and completely obliterated learning to an air-puff US (Figs. 6 and 7). The complete absence of learning to a sensory US in these animals was particularly surprising given the relative subtlety of the effects on complex spiking (Fig. 7), and the ability of these mice to learn to an optogenetic CF-US (Fig. 1). Moreover, the effect was exquisitely sensitive to ChR2 expression levels – a 5-fold reduction in viral titer was enough to restore both normal complex spiking and learning to an air-puff US (Figs. 6 and 7).

Climbing fiber ChR2 expression provided an unexpectedly selective tool for reducing evoked complex spikes, with no measurable effect on Purkinje cell simple spikes and only subtle reductions in spontaneous complex spiking. For our purposes, this unexpected effect was serendipitous, as it provided an unparalleled opportunity to assess the contributions of

climbing fiber signaling to cerebellar learning. However, the discovery that simple ChR2 expression can have drastic behavioral consequences has important implications for experiments using optogenetic circuit dissection more broadly. It is well known that expression of ChR2 and other membrane proteins can alter neuronal morphology and physiology[68–70] in ways that are still not fully understood. It is possible that IO neurons may be particularly vulnerable, for example due to their high levels of electrical coupling[53,71]. It is also possible that the use of the CaMKIIa promoter contributed in this case, either by driving particularly strong expression levels[70] or through perturbing endogenous CaMKII function in the IO[72]. However, the effects on complex spiking we observed were not immediately obvious, and required painstaking quantitative analysis. We were only able to identify them and link them to their dramatic behavioral consequences because cell-type specific activity patterns in the cerebellar circuit and their relationship to relevant sensorimotor signals have previously been exceptionally well characterized. Thus, although they solve one problem for the cerebellum, our findings also highlight the major challenge of identifying and fully characterizing circuit tools that allow for selective and predictable manipulation of specific neural signals within complex networks.

**Conclusion and outlook for cerebellar learning**
Our findings raise important questions about how sensorimotor errors are encoded in the cerebellum to support a full range of cerebellum-dependent behaviors.

First, while our results reveal a necessary role for climbing fiber-driven Purkinje cell complex spikes in eyeblink conditioning, they do not rule out a possible role for additional plasticity mechanisms in the cerebellar nuclei, which may be important for some components of learning. Previous work has suggested that cerebellar learning may consist of multiple stages, with initial learning in the cerebellar cortex (driven mainly by CF inputs) leading to changes in Purkinje cell output that then sculpt plasticity in the cerebellar nuclei[4,73]. The relative contributions of cortical vs. nuclear plasticity may vary across stages of learning, or for different forms of cerebellar learning that progress on different time scales – from short-term motor adaptation over seconds and minutes[15,74], to eyeblink conditioning which takes days[75], to long-term motor adaptation after prolonged wearing of prism goggles[76], for example.

Second, we cannot exclude the possibility that parallel fiber inputs may provide instructive signals independent of climbing fiber input for other forms of cerebellar learning. For instance, whole body movements like locomotion generate robust activation of mossy fiber inputs[77,78]. There is evidence that coincident input from spatially clustered parallel fibers can elicit dendritic calcium events in Purkinje cells[79–81], which could drive cerebellar plasticity in the absence of climbing fiber inputs[82,83]. It is therefore possible that during some cerebellum-dependent forms of motor adaptation[84–86], sufficiently high levels of parallel fiber activation could instruct parallel fiber plasticity.

Regardless of possible contributions from additional mechanisms, our findings establish climbing fiber instructive signals as an essential component of associative cerebellar learning. In considering whether a similar requirement might hold across various forms of cerebellum-dependent learning, we note the remarkable quantitative correspondence between the complex spike probability-based learning thresholds we observed here, and that predicted by electrophysiological recordings during trial-to-trial learning in primate smooth pursuit eye movements[15,87]. Results from both systems indicate that learning drops off sharply when CSpk probabilities in response to an instructive stimulus fall below ~0.3

11

(Figs. 6-7). This sharp dropoff is particularly striking given that complex spikes are not exclusively driven by sensorimotor errors[18,32,88], and that CSpk probabilities in response to even the strongest behavioral instructive signals can be fairly low[13,15,85–87,89,90]. It is intriguing to speculate that this quantitative correspondence could hint at a generality of mechanism of action for the enigmatic Purkinje cell complex spike.

12

## METHODS

### Animals

All procedures were carried out in accordance with the European Union Directive 86/609/EEC and approved by the Champalimaud Centre for the Unknown Ethics Committee and the Portuguese Direção Geral de Veterinária (Ref. No. 0421/000/000/2015). Mice were kept on a reversed 12-h light/12-h dark cycle with food and water ad libitum. All procedures were performed in male and female mice of approximately 12–14 weeks of age. The animals that were injected with AAV had an additional waiting period of 6 weeks before the start of experiments.

*Mouse lines*. WT C57BL/6J mice were obtained from The Jackson Laboratory (strain #000664). Selective ChR2 expression in Purkinje cells (*L7-Cre;ChR2*; Figs. 2, 3, Supp. Fig 2), granule cells (*Gabra6-Cre;ChR2*; Fig. 4), and glutamatergic neurons within the IO (*vGlut2-Cre;ChR2*; Supp. Fig. 1; Fig. 5) were obtained by crossing specific Cre driver lines with ChR2-EYFP-LoxP mice (strain #012569 from The Jackson Laboratory; [91]) to generate cell-type specific ChR2-expressing transgenic animals (Supp. Table 1). Cre lines were: For Purkinje cells*,* L7-Cre strain #004146 from The Jackson Laboratory[51,92]; For granule cells, Gabra6-Cre (MMRRC 000196-UCD; [51,52,93,94]); For glutamatergic neurons (within the IO), vGlut2-Cre (strain #016963 from The Jackson Laboratory; [57,95,96]). To target inputs to the IO, we used the Thy1-ChR2/EYFP mouse line obtained from The Jackson Laboratory[65,66] (strain #007612).

### Surgical procedures

For all surgeries, animals were anesthetized with isoflurane (4% induction and 0.5 – 1.5% for maintenance), placed in a stereotaxic frame (David Kopf Instruments, Tujunga, CA) and a custom-cut metal head plate was glued to the skull with dental cement (Super Bond – C&B). At the end of the surgery, mice were also administered a non-steroidal anti-inflammatory and painkiller drug (Carprofen). After all surgical procedures, mice were monitored and allowed ~1-2 days of recovery.

*Viral injections*. Climbing fibers (CF) were targeted[26,50] by injecting 250nl of AAV1.CaMKIIa.hChR2(H134R)-mCherry.WPRE.hGH (Addgene#26975; [97]) at the left dorsal accessory inferior olive (IO), which has been previously implicated in eyeblink conditioning (RC -6.3, ML -0.5, DV 5.55; [23,24,26]). We initially (Fig. 1, Supp. Fig. 1, Fig. 6a-d) diluted the stock virus 1:10 in ACSF to yield a final titer of $1,31 \times 10^{12}$ GC/ml, in line with previous studies [26]. For the low-expression conditions in Figs. 6 and 7 (CF-ChR2-LE; Supp. Table 1) we diluted the virus an additional 5x to yield a final titer of $2,62 \times 10^{11}$ GC/ml. CF-ChR2 mice started the behavioral and electrophysiological experiments 6 weeks after injection to allow time for virus expression and stabilization[26].

| Fig # | Experimental condition | Expression strategy | Mouse genotype | Virus | Promoter | Cell type targeted | Fiber placement |
|---|---|---|---|---|---|---|---|
| 1, 6, 7 | **CF-ChR2-Ctx** | viral | wt(C57Bl6) | AAV-CamKII-ChR2 (10^12) | CaMKII | **CF** | **Ctx** |
| 1, 6, 7 | **CF-ChR2-IO** | viral | wt(C57Bl6) | AAV-CamKII-ChR2 (10^12) | CaMKII | **CF** | **IO** |
| 2, 3, Supp. 2 | **Pkj-ChR2** | transgenic | L7-Cre;ChR2 | | L7 | **Pkj** | Ctx |
| 4 | **Gabra6-ChR2-Ctx** | transgenic | Gabra6-Cre;ChR2 | | **Gabra6** | granule cells | **Ctx** |
| 5, Supp. 1 | **vGlut2-ChR2-IO** | transgenic | vGlut2-Cre;ChR2 | | **vGlut2** | IO-glut | **IO** |
| 5 | **Thy1-ChR2-IO** | transgenic | Thy1-ChR2 | | **Thy1** | IO-inputs | **IO** |
| 6, 7, Supp. 3 | **CF-ChR2-LE** | viral | wt(C57Bl6) | AAV-CamKII-ChR2 (10^11) | CaMKII | **CF** | IO |

**Supp. Table 1.** *Summary of genetic and anatomical targeting approaches used for selective targeting of individual cerebellar circuit elements.*

For optogenetic manipulations (Supp. Table 1), optical fibers with 100µm core diameter, 0.22 NA (Doric lenses, Quebec, Canada) were lowered into the brain through small craniotomies performed with a dental drill, and positioned at either the right cerebellar cortical eyelid region (RC -5.7, ML +1.9, DV -1.5)[53,54,56] or at the left dorsal accessory inferior olive (IO; RC -6.3, ML -0.5, DV -5.5), which has been previously implicated in eyeblink conditioning [23,24,98]. Correct fiber placement in both the cerebellar cortex and IO was functionally verified before experiments by the presence of an evoked eyeblink in the right eye with moderate intensity (see below) laser stimulation and subsequently confirmed histologically.

For in vivo electrophysiological recordings, a disposable 3 mm biopsy punch was used to perform a craniotomy over the right cerebellar cortical eyelid region (RC -5.7, ML +1.9; [53,54,56]. The craniotomy was covered with a 3mm glass coverslip with 4 small holes where the electrode could pass through, and then by a silicon based elastomer (Kwik-cast, WPI) that was easily removed just before recording sessions.

**Behavioral procedures**

The experimental setup for eyeblink conditioning was based on previous work[51,52]. For all behavioral experiments, mice head-fixed and walking on a Fast-Trac Activity Wheel (Bio-Serv). A DC motor with an encoder (Maxon) was used to externally control the speed of the treadmill. Mice were habituated to the behavioral setup for at least 4 days prior to training, until they walked normally at the target speed of 0.1m/s and displayed no external signs of distress. Eyelid movements of the right eye were recorded using a high-speed monochromatic camera (Genie HM640, Dalsa) to monitor a 172x160 pixel region at 900fps. Custom-written LabVIEW software, together with a NI PCIE-8235 frame grabber and a NI-DAQmx board (National Instruments), was used to synchronously trigger and control the hardware.

Acquisition sessions consisted of the presentation of 90 CS+US paired trials and 10 CS-only trials. The 100 trials were separated by a randomized inter trial interval (ITI) of 10-15s. Unless otherwise stated, CS and US onsets on CS+US paired trials were separated by a fixed inter-stimulus interval (ISI) of 300ms and both stimuli co-terminated. The CS was a white light LED positioned ~3cm directly in front of the mouse. The sensory unconditioned stimulus (US) was an air-puff (40psi, 50ms) controlled by a Picospritzer (Parker) and delivered via a 27G needle positioned ~0.5cm away from the cornea of the right eye of the mouse. Air-puff direction was adjusted for each session of each mouse so that the US elicited a strong reflexive eye blink unconditioned response (UR).

*Behavioral analysis.* Videos from each trial were analyzed offline with custom-written MATLAB (MathWorks) software [51]. Distance between eyelids was calculated frame by frame by thresholding the grayscale image and extracting the minor axis of the ellipse that delineated the eye. Eyelid traces were normalized for each session, from 0 (maximal opening of the eye throughout the session) to 1 (full eye closure achieved under air-puff treatment). Trials were classified as containing CRs if an eyelid closure with normalized amplitude >0.1 occurred >100ms after CS onset and before US onset.

**Optogenetic stimulation**

Light from 473 nm lasers (LRS-0473-PFF-00800-03, LaserGlow Technologies) was controlled with custom-written LabView code. Predicted irradiance levels for the 100um diameter, 0.22NA optical cannulas used in our study was calculated using the online platform: https://web.stanford.edu/group/dlab/optogenetics. All laser powers are comparable to those of previous studies[26,27,49–51,54,65].

For Pkj-ChR2 (Figs. 2 and 3), Gabra6-ChR2 (Fig. 4) and vGlut2-ChR2-IO and Thy1-ChR2-IO (Fig. 5) experiments, laser power was adjusted for each mouse and controlled for each experiment using a light power meter (Thorlabs) at the beginning and end of each session. For the Pkj-ChR2 experiments of Fig. 2, Fig. 3a-i, and Supp. Fig 2b-d, laser intensity was adjusted to elicit an intermediate eyelid closure at stimulus offset (1-3mW, max irradiance of 95.5mW/mm^2. For the Pkj-ChR2-high (blink at laser onset) experiments of Fig. 3j-m and Supp. Fig. 2e-h powers ranged from 8-12mW, max irradiance of 381.8mW/mm^2. For the Gabra6-ChR2 experiments of Fig. 4, intensities were up to 6mW, irradiance of 190.9mW/mm^2). For the vGlut2-ChR2-IO and Thy1-ChR2-IO perturbation experiments of Fig. 5, laser power was lowered to comfortably below the threshold for detectable eyelid movement (vGlut2-ChR2-IO: 1-3.3mW; Thy1-ChR2-IO: 2.3-3.3mW, max predicted irradiance of 105mW/mm^2).

For the CF-ChR2 experiments of Fig. 1 and 6, since these animals did not blink to laser stimulation (Supp. Fig. 1h), the power was set to 6mW, max irradiance of 190.9mW/mm^2). This power was confirmed with electrophysiology to reliably drive Purkinje cell complex spikes. The same power was also used for all CF-ChR2-LE experiments; these animals exhibited a small eyelid twitch in response to laser stimulation (Fig. 6g).

When optogenetic stimulation was substituted for a sensory US, where possible we adjusted the timing (onset and duration) of the laser stimulation so that the reflexive blinks would most closely match those elicited by a sensory US (50ms air-puff delivered to the eye). For Pkj-ChR2 and Gabra6-ChR2 experiments, 100ms laser stimulation best elicited a blink similar to that of the airpuff. Because Pkj-ChR2-med stimulation elicits a blink at the offset of laser stimulation, whereas GC-ChR2 elicits a blink at the onset of laser stimulation (due to Purkinje cell inhibition via molecular layer interneurons), the onset of the laser stimulation was also adjusted specifically for those experiments. For the CF-ChR2 experiments of Fig. 1, since there was no laser-driven blink (Supp. Fig. 1h), we kept the 100ms laser duration and matched the timing of laser stimulation/ complex spike onset.

## Electrophysiological recordings

All recordings were performed in vivo, in awake mice. Cell-attached single-cell recordings were made using long-shanked borosilicate glass pipettes (Warner Instruments) pulled on a vertical puller (Narishige PC-100) and filled with saline solution (0.9% NaCl, typical resistances between 4-5 MΩ). An Optopatcher (A-M Systems) was used for simultaneous optogenetic stimulation and electrophysiological recordings. Laser light (with the same blue laser used for the behavioral optogenetic manipulations) was transmitted through an optic fiber (50 μm core diameter) inserted inside the glass pipette until it could fit, ~5 mm from the tip. The Optopatcher was oriented towards the cerebellar eyeblink region with a motorized 4-axis micromanipulator (PatchStar, Scientifica). Craniotomies were filled with saline and connected to the ground reference using a silver-chloride pellet (Molecular Devices).

Recordings were performed with a Multiclamp 700B amplifier (Axon Instruments) in its voltage-clamp configuration, with a gain of 0.5 V/nA and low-pass Bessel filter with 10 kHz cut-off. The current offset between the interior and exterior of the pipette was always kept neutral to avoid passive stimulation of the cells. All recordings were sampled at 25kHz from the output signal of the amplifier using a NI-DAQmx board and Labview custom-software. Purkinje cells were identified by the presence of complex spikes. In cells that exhibited spontaneous complex spikes (a typical criterion for identifying Purkinje cells in electrophysiological recordings), we observed subtly lower spontaneous complex spike rates in Purkinje cells of CF-ChR2 mice compared to controls. Because of this, for all CF-ChR2 (and CF-ChR2-LE) experiments, Purkinje cells were identified based on the presence of a laser-triggered complex spike rather than spontaneous complex spikes, to avoid selection bias resulting from the absence of spontaneous complex spiking (Fig. 7). Spikes were sorted offline using custom Python code for simple spikes and a modified Un'Eye neural network[99] for complex spikes.

## Histology

After the experiments, animals were perfused transcardially with 4% paraformaldehyde and their brains removed. Brain sections (50um thick) were cut in a vibratome and stained for Purkinje cells (with chicken anti-calbindin primary antibody #214006 SYSY, and anti-chicken Alexa488 #703-545-155 or Alexa594 #703-545-155 secondary antibodies from Jackson Immunoresearch) and for cell viability (with DAPI marker). Brain sections were then mounted on glass slides with mowiol mounting medium, and imaged with 5x, 10x or 20x objectives. Brain preparations from experiments where Climbing Fibers were specifically targeted were also imaged with an upright confocal laser point-scanning microscope (Zeiss LSM 710), using a 10x or 40x objective.

## Statistical analysis

Data are reported as mean ± s.e.m., and statistical analyses were performed using the Statistics toolbox in MATLAB. A Two-sample t-Test was performed for all comparisons unless otherwise indicated. Differences were considered significant at *$P<0.05$, **$P<0.01$, and ***$P<0.001$. No statistical methods were used to predetermine sample sizes; sample sizes are similar to those reported in previous publications [51,52,54]. Data collection and analysis were not performed blind to the conditions of the experiments. Mice were randomly assigned to specific experimental groups without bias.

## REFERENCES

1.  Marr, D. A theory of cerebellar cortex. *J. Physiol.* **202**, 437–470 (1969).
2.  Albus, J. S. A theory of cerebellar function. *Math. Biosci.* **10**, 25–61 (1971).
3.  Ito, M. Neural design of the cerebellar motor control system. *Brain Res.* **40**, 81–84 (1972).
4.  Raymond, J. L., Lisberger, S. G. & Mauk, M. D. The cerebellum: a neuronal learning machine? *Science* **272**, 1126–1131 (1996).
5.  Medina, J. F., Garcia, K. S., Nores, W. L., Taylor, N. M. & Mauk, M. D. Timing Mechanisms in the Cerebellum: Testing Predictions of a Large-Scale Computer Simulation. *J. Neurosci.* **20**, 5516 LP – 5525 (2000).
6.  De Zeeuw, C. I. & Yeo, C. H. Time and tide in cerebellar memory formation. *Curr. Opin. Neurobiol.* **15**, 667–674 (2005).
7.  Raymond, J. L. & Medina, J. F. Computational Principles of Supervised Learning in the Cerebellum. *Annu. Rev. Neurosci.* **41**, 233–253 (2018).
8.  Lisberger, S. G. The Rules of Cerebellar Learning: Around the Ito Hypothesis. *Neuroscience* **462**, 175–190 (2021).
9.  Ito, M. & Kano, M. Long-lasting depression of parallel fiber-Purkinje cell transmission induced by conjunctive stimulation of parallel fibers and climbing fibers in the cerebellar cortex. *Neurosci. Lett.* **33**, 253–258 (1982).
10. Schmolesky, M., Weber, J., de Zeeuw, C. & Hansel, C. The making of a complex spike: Ionic composition and plasticity. (2002) doi:10.1111/j.1749-6632.2002.tb07581.x.
11. Coesmans, M., Weber, J. T., De Zeeuw, C. I. & Hansel, C. Bidirectional parallel fiber plasticity in the cerebellum under climbing fiber control. *Neuron* **44**, 691–700 (2004).
12. Carey, M. R. Synaptic mechanisms of sensorimotor learning in the cerebellum. *Curr. Opin. Neurobiol.* **21**, 609–615 (2011).
13. Gilbert, P. F. & Thach, W. T. Purkinje cell activity during motor learning. *Brain Res.* **128**, 309–328 (1977).
14. Sears, L. L. & Steinmetz, J. E. Acquisition of classically conditioned-related activity in the hippocampus is affected by lesions of the cerebellar interpositus nucleus. *Behavioral Neuroscience* vol. 104 681–692 (1990).
15. Medina, J. F. & Lisberger, S. G. Links from complex spikes to local plasticity and motor learning in the cerebellum of awake-behaving monkeys. *Nat. Neurosci.* **11**, 1185–1192 (2008).
16. Rasmussen, A., Jirenhed, D.-A., Wetmore, D. Z. & Hesslow, G. Changes in complex spike activity during classical conditioning. *Front. Neural Circuits* **8**, 90 (2014).
17. Kimpo, R. R., Rinaldi, J. M., Kim, C. K., Payne, H. L. & Raymond, J. L. Gating of neural error signals during motor learning. *Elife* **3**, e02076–e02076 (2014).
18. Ohmae, S. & Medina, J. F. Climbing fibers encode a temporal-difference prediction error during cerebellar learning in mice. *Nat. Neurosci.* **18**, 1798–1803 (2015).
19. Stone, L. S. & Lisberger, S. G. Visual responses of Purkinje cells in the cerebellar flocculus during smooth-pursuit eye movements in monkeys. II. Complex spikes. *J. Neurophysiol.* **63**, 1262–1275 (1990).
20. Kahlon, M. & Lisberger, S. G. Coordinate system for learning in the smooth pursuit eye movements of monkeys. *J. Neurosci.* **16**, 7270–7283 (1996).
21. Kim, J. J., Krupa, D. J. & Thompson, R. F. Inhibitory cerebello-olivary projections and blocking effect in classical conditioning. *Science* **279**, 570–573 (1998).
22. Medina, J. F., Nores, W. L. & Mauk, M. D. Inhibition of climbing fibres is a signal for the extinction of conditioned eyelid responses. *Nature* **416**, 330–333 (2002).
23. Kim, O. A., Ohmae, S. & Medina, J. F. A cerebello-olivary signal for negative prediction error is sufficient to cause extinction of associative motor learning. *Nat. Neurosci.* **23**, 1550–1554 (2020).
24. Mauk, M. D., Steinmetz, J. E. & Thompson, R. F. Classical conditioning using stimulation of the inferior olive as the unconditioned stimulus. *Proc. Natl. Acad. Sci. U. S. A.* **83**, 5349–5353 (1986).
25. Steinmetz, J. E., Lavond, D. G. & Thompson, R. F. Classical conditioning in rabbits using pontine nucleus stimulation as a conditioned stimulus and inferior olive stimulation as an unconditioned stimulus. *Synapse* **3**, 225–233 (1989).
26. Nguyen-Vu, T. D. B. *et al.* Cerebellar Purkinje cell activity drives motor learning. *Nat. Neurosci.* **16**, 1734–1736 (2013).

27. Rowan, M. J. M. *et al.* Graded Control of Climbing-Fiber-Mediated Plasticity and Learning by Inhibition in the Cerebellum. *Neuron* **99**, 999-1015.e6 (2018).

28. Zbarska, S., Bloedel, J. R. & Bracha, V. Cerebellar Dysfunction Explains the Extinction-Like Abolition of Conditioned Eyeblinks After NBQX Injections in the Inferior Olive. *J. Neurosci.* **28**, 10 LP – 20 (2008).

29. Ke, M. C., Guo, C. C. & Raymond, J. L. Elimination of climbing fiber instructive signals during motor learning. *Nat. Neurosci.* **12**, 1171–1179 (2009).

30. Schonewille, M. *et al.* Reevaluating the Role of LTD in Cerebellar Motor Learning. *Neuron* **70**, 43–50 (2011).

31. Popa, L. S., Streng, M. L., Hewitt, A. L. & Ebner, T. J. The Errors of Our Ways: Understanding Error Representations in Cerebellar-Dependent Motor Learning. *The Cerebellum* **15**, 93–103 (2016).

32. Streng, M. L., Popa, L. S. & Ebner, T. J. Complex Spike Wars: a New Hope. *The Cerebellum* **17**, 735–746 (2018).

33. Sanger, T. D. & Kawato, M. A Cerebellar Computational Mechanism for Delay Conditioning at Precise Time Intervals. *Neural Comput.* **32**, 2069–2084 (2020).

34. McCormick, D. A., Steinmetz, J. E. & Thompson, R. F. Lesions of the inferior olivary complex cause extinction of the classically conditioned eyeblink response. *Brain Res.* **359**, 120–130 (1985).

35. Luebke, A. E. & Robinson, D. A. Gain changes of the cat's vestibulo-ocular reflex after flocculus deactivation. *Exp. brain Res.* **98**, 379–390 (1994).

36. Zucca, R., Rasmussen, A. & Bengtsson, F. Climbing Fiber Regulation of Spontaneous Purkinje Cell Activity and Cerebellum-Dependent Blink Responses(1,2,3). *eNeuro* **3**, (2016).

37. Lang, E. J. *et al.* The Roles of the Olivocerebellar Pathway in Motor Learning and Motor Control. A Consensus Paper. *The Cerebellum* **16**, 230–252 (2017).

38. Miles, F. A. & Lisberger, S. G. Plasticity in the vestibulo-ocular reflex: a new hypothesis. *Annu. Rev. Neurosci.* **4**, 273–299 (1981).

39. Kawato, M., Furukawa, K. & Suzuki, R. A hierarchical neural-network model for control and learning of voluntary movement. *Biol. Cybern.* **57**, 169–185 (1987).

40. du Lac, S. & Lisberger, S. G. Cellular processing of temporal information in medial vestibular nucleus neurons. *J. Neurosci.* **15**, 8000 LP – 8010 (1995).

41. Raymond, J. L. & Lisberger, S. G. Neural Learning Rules for the Vestibulo-Ocular Reflex. *J. Neurosci.* **18**, 9112 LP – 9129 (1998).

42. Carey, M. R., Medina, J. F. & Lisberger, S. G. Instructive signals for motor learning from visual cortical area MT. *Nat. Neurosci.* **8**, 813–819 (2005).

43. Shin, S.-L., Zhao, G. Q. & Raymond, J. L. Signals and Learning Rules Guiding Oculomotor Plasticity. *J. Neurosci.* **34**, 10635 LP – 10644 (2014).

44. Albert, S. T. & Shadmehr, R. The Neural Feedback Response to Error As a Teaching Signal for the Motor Learning System. *J. Neurosci.* **36**, 4832 LP – 4845 (2016).

45. Popa, L. S., Hewitt, A. L. & Ebner, T. J. Predictive and Feedback Performance Errors Are Signaled in the Simple Spike Discharge of Individual Purkinje Cells. *J. Neurosci.* **32**, 15345 LP – 15358 (2012).

46. Lisberger, S. G. & Fuchs, A. F. Role of primate flocculus during rapid behavioral modification of vestibuloocular reflex. I. Purkinje cell activity during visually guided horizontal smooth-pursuit eye movements and passive head rotation. *J. Neurophysiol.* **41**, 733–763 (1978).

47. Pugh, J. R. & Raman, I. M. Nothing can be coincidence: Synaptic inhibition and plasticity in the cerebellar nuclei. *Trends in Neurosciences* vol. 32 170–177 (2009).

48. McElvain, L. E., Bagnall, M. W., Sakatos, A. & du Lac, S. Bidirectional plasticity gated by hyperpolarization controls the gain of postsynaptic firing responses at central vestibular nerve synapses. *Neuron* **68**, 763–775 (2010).

49. Lee, K. H. *et al.* Circuit Mechanisms Underlying Motor Memory Formation in the Cerebellum. *Neuron* **86**, 529–540 (2015).

50. Bonnan, A., Rowan, M. M. J., Baker, C. A., Bolton, M. M. & Christie, J. M. Autonomous Purkinje cell activation instructs bidirectional motor learning through evoked dendritic calcium signaling. *Nat. Commun.* **12**, 2153 (2021).

51. Albergaria, C., Silva, N. T., Pritchett, D. L. & Carey, M. R. Locomotor activity modulates associative learning in mouse cerebellum. *Nat. Neurosci.* **21**, 725–735 (2018).

52. Albergaria, C., Silva, N. T., Darmohray, D. M. & Carey, M. R. Cannabinoids modulate

associative cerebellar learning via alterations in behavioral state. *Elife* **9**, e61821 (2020).

53. Van Der Giessen, R. S. *et al.* Role of Olivary Electrical Coupling in Cerebellar Motor Learning. *Neuron* **58**, 599–612 (2008).

54. Heiney, S. A., Kim, J., Augustine, G. J. & Medina, J. F. Precise Control of Movement Kinematics by Optogenetic Inhibition of Purkinje Cell Activity. *J. Neurosci.* **34**, 2321 LP – 2330 (2014).

55. Mostofi, A., Holtzman, T., Grout, A. S., Yeo, C. H. & Edgley, S. A. Electrophysiological Localization of Eyeblink-Related Microzones in Rabbit Cerebellar Cortex. *J. Neurosci.* **30**, 8920 LP – 8934 (2010).

56. Steinmetz, A. B. & Freeman, J. H. Localization of the cerebellar cortical zone mediating acquisition of eyeblink conditioning in rats. *Neurobiol. Learn. Mem.* **114**, 148–154 (2014).

57. Hioki, H. *et al.* Differential distribution of vesicular glutamate transporters in the rat cerebellar  cortex. *Neuroscience* vol. 117 1–6 (2003).

58. Perrett, S. P., Ruiz, B. P. & Mauk, M. D. Cerebellar cortex lesions disrupt learning-dependent timing of conditioned eyelid  responses. *J. Neurosci.* **13**, 1708–1718 (1993).

59. Chettih, S. N., McDougle, S. D., Ruffolo, L. I. & Medina, J. F. Adaptive timing of motor output in the mouse: the role of movement oscillations in eyelid conditioning. *Front. Integr. Neurosci.* **5**, 72 (2011).

60. Gauck, V. & Jaeger, D. The Control of Rate and Timing of Spikes in the Deep Cerebellar Nuclei by Inhibition. *J. Neurosci.* **20**, 3006 LP – 3016 (2000).

61. Garcia, K. S., Steele, P. M. & Mauk, M. D. Cerebellar Cortex Lesions Prevent Acquisition of Conditioned Eyelid Responses. *J. Neurosci.* **19**, 10940 LP – 10947 (1999).

62. Herman, A. M., Huang, L., Murphey, D. K., Garcia, I. & Arenkiel, B. R. Cell type-specific and time-dependent light exposure contribute to silencing in neurons expressing Channelrhodopsin-2. *Elife* **3**, e01481 (2014).

63. Kruse, W. *et al.* Optogenetic Modulation and Multi-Electrode Analysis of Cerebellar Networks In Vivo. *PLoS One* **9**, e105589 (2014).

64. Dittman, J. S. & Regehr, W. G. Calcium Dependence and Recovery Kinetics of Presynaptic Depression at the Climbing Fiber to Purkinje Cell Synapse. *J. Neurosci.* **18**, 6147 LP – 6162 (1998).

65. Arenkiel, B. R. *et al.* In Vivo Light-Induced Activation of Neural Circuitry in Transgenic Mice Expressing Channelrhodopsin-2. *Neuron* **54**, 205–218 (2007).

66. Garden, D. L. F., Rinaldi, A. & Nolan, M. F. Active integration of glutamatergic input to the inferior olive generates bidirectional postsynaptic potentials. *J. Physiol.* **595**, 1239–1251 (2017).

67. Aschauer, D. F., Kreuz, S. & Rumpel, S. Analysis of Transduction Efficiency, Tropism and Axonal Transport of AAV Serotypes 1, 2, 5, 6, 8 and 9 in the Mouse Brain. *PLoS One* **8**, e76310 (2013).

68. Zimmermann, D. *et al.* Effects on capacitance by overexpression of membrane proteins. *Biochem. Biophys. Res. Commun.* **369**, 1022–1026 (2008).

69. Lin, J. Y. Chapter 2 - Optogenetic excitation of neurons with channelrhodopsins: Light instrumentation, expression systems, and channelrhodopsin variants. in *Optogenetics: Tools for Controlling and Monitoring Neuronal Activity* (eds. Knöpfel, T. & Boyden, E. S. B. T.-P. in B. R.) vol. 196 29–47 (Elsevier, 2012).

70. Miyashita, T., Shao, Y., Chung, J., Pourzia, O. & Feldman, D. Long-term channelrhodopsin-2 (ChR2) expression can induce abnormal axonal morphology and targeting in cerebral cortex   . *Frontiers in Neural Circuits*   vol. 7 (2013).

71. Garden, D. L. F. *et al.* Inferior Olive HCN1 Channels Coordinate Synaptic Integration and Complex Spike Timing. *Cell Rep.* **22**, 1722–1733 (2018).

72. Bazzigaluppi, P. *et al.* Modulation of Murine Olivary Connexin 36 Gap Junctions by PKA and CaMKII   . *Frontiers in Cellular Neuroscience*   vol. 11 (2017).

73. Kassardjian, C. D. *et al.* The Site of a Motor Memory Shifts with Consolidation. *J. Neurosci.* **25**, 7979 LP – 7985 (2005).

74. Yang, Y. & Lisberger, S. G. Learning on Multiple Timescales in Smooth Pursuit Eye Movements. *J. Neurophysiol.* **104**, 2850–2862 (2010).

75. Medina, J. F., Garcia, K. S. & Mauk, M. D. A Mechanism for Savings in the Cerebellum. *J. Neurosci.* **21**, 4081 LP – 4089 (2001).

76. Lisberger, S. G. Neural basis for motor learning in the vestibuloocular reflex of primates. III. Computational and behavioral analysis of the sites of learning. *J. Neurophysiol.* **72**, 974–998 (1994).

77.  Powell, K., Mathy, A., Duguid, I. & Häusser, M. Synaptic representation of locomotion in single cerebellar granule cells. *Elife* **4**, e07290 (2015).

78.  Ishikawa, T., Shimuta, M. & Häusser, M. Multimodal sensory integration in single cerebellar granule cells in vivo. *Elife* **4**, e12916 (2015).

79.  Wang, Y. T. & Linden, D. J. Expression of Cerebellar Long-Term Depression Requires Postsynaptic Clathrin-Mediated Endocytosis. *Neuron* **25**, 635–647 (2000).

80.  Roome, C. J. & Kuhn, B. Simultaneous dendritic voltage and calcium imaging and somatic recording from Purkinje neurons in awake mice. *Nat. Commun.* **9**, 3388 (2018).

81.  Roome, C. J. & Kuhn, B. Dendritic coincidence detection in Purkinje neurons of awake mice. *Elife* **9**, e59619 (2020).

82.  Hartell. Strong Activation of Parallel Fibers Produces Localized Calcium Transients and a Form of LTD That Spreads to Distant Synapses. *Neuron* **16**, 601–610 (1996).

83.  Hartell. Parallel fiber plasticity. *The Cerebellum* **1**, 3–18 (2002).

84.  Darmohray, D. M., Jacobs, J. R., Marques, H. G. & Carey, M. R. Spatial and Temporal Locomotor Learning in Mouse Cerebellum. *Neuron* **102**, 217-231.e4 (2019).

85.  Herzfeld, D. J., Kojima, Y., Soetedjo, R. & Shadmehr, R. Encoding of action by the Purkinje cells of the cerebellum. *Nature* **526**, 439–442 (2015).

86.  Herzfeld, D. J., Kojima, Y., Soetedjo, R. & Shadmehr, R. Encoding of error and learning to correct that error by the Purkinje cells of the cerebellum. *Nat. Neurosci.* **21**, 736–743 (2018).

87.  Herzfeld, D. J., Hall, N. J., Tringides, M. & Lisberger, S. G. Principles of operation of a cerebellar learning circuit. *Elife* **9**, e55217 (2020).

88.  Hull, C. Prediction signals in the cerebellum: Beyond supervised motor learning. *Elife* **9**, e54073 (2020).

89.  Yang, Y. & Lisberger, S. G. Purkinje-cell plasticity and cerebellar motor learning are graded by complex-spike duration. *Nature* **510**, 529–532 (2014).

90.  Yang, Y. & Lisberger, S. G. Interaction of plasticity and circuit organization during the acquisition of cerebellum-dependent motor learning. *Elife* **2**, e01574 (2013).

91.  Madisen, L. *et al.* A toolbox of Cre-dependent optogenetic transgenic mice for light-induced activation and silencing. *Nat. Neurosci.* **15**, 793–802 (2012).

92.  Barski, J. J., Dethleffsen, K. & Meyer, M. Cre recombinase expression in cerebellar Purkinje cells. *genesis* **28**, 93–98 (2000).

93.  Fünfschilling, U. & Reichardt, L. F. Cre-mediated recombination in rhombic lip derivatives. *genesis* **33**, 160–169 (2002).

94.  Carey, M. R. *et al.* Presynaptic CB1 Receptors Regulate Synaptic Plasticity at Cerebellar Parallel Fiber Synapses. *J. Neurophysiol.* **105**, 958–963 (2010).

95.  Fremeau, R. T. *et al.* The Expression of Vesicular Glutamate Transporters Defines Two Classes of Excitatory Synapse. *Neuron* **31**, 247–260 (2001).

96.  Borgius, L., Restrepo, C. E., Leao, R. N., Saleh, N. & Kiehn, O. A transgenic mouse line for molecular genetic analysis of excitatory glutamatergic neurons. *Mol. Cell. Neurosci.* **45**, 245–257 (2010).

97.  Lee, J. H. *et al.* Global and local fMRI signals driven by neurons defined optogenetically by type and wiring. *Nature* **465**, 788–792 (2010).

98.  De Zeeuw, C. I., Wentzel, P. & Mugnaini, E. Fine structure of the dorsal cap of the inferior olive and its GAB aergic and non-Gabaergic input from the nucleus prepositus hypoglossi in rat and rabbit. *J. Comp. Neurol.* **327**, 63–82 (1993).

99.  Markanday, A. *et al.* Using deep neural networks to detect complex spikes of cerebellar Purkinje cells. *J. Neurophysiol.* **123**, 2217–2234 (2020).
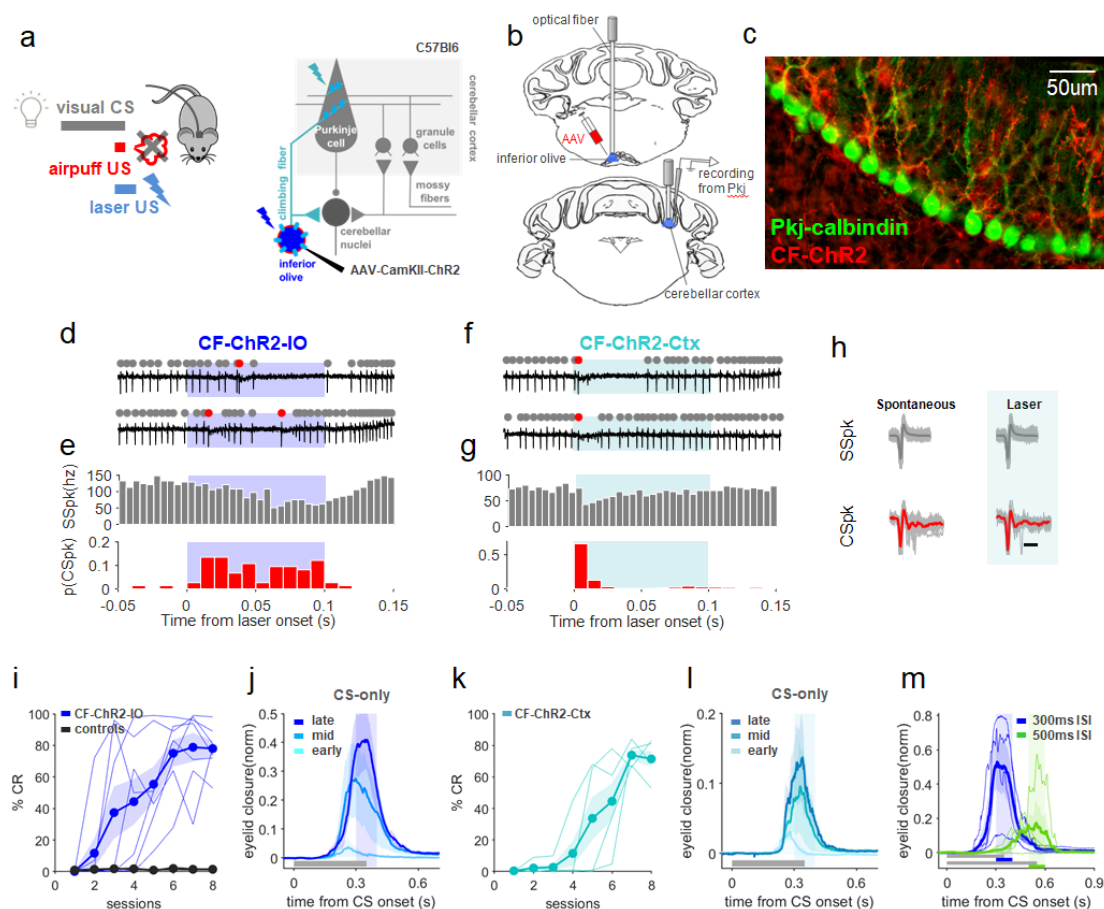
## FIGURES



**Fig.1. Optogenetic climbing fiber stimulation instructs eyeblink conditioning.**
**a**, Left, experimental scheme of delay eyeblink conditioning to an optogenetic US. The traditional airpuff US is replaced by laser stimulation and paired with a visual CS. Right, cerebellar circuit underlying eyeblink conditioning and experimental strategy. Wild-type animals were injected with a AAV-CamKII-ChR2 in the IO and differential sites of photoactivation were used to photoactivate climbing fiber somas (blue) or terminals in the cerebellar cortex (cyan). **b**, Optical fibers were implanted in either the left IO or the eyelid region of the right cerebellar cortex, where single-unit recordings were performed from Purkinje cells. **c**, Example sagittal section of cerebellar cortex. ChR2 (red) is expressed in climbing fiber inputs to Purkinje cells (green). (Also see Supp. Fig. 1) **d**, Two example electrophysiological traces from a Purkinje cell with identified simple spikes (grey dots) and complex spikes (red dots) in response to CF-ChR2 laser stimulation in the IO (CF-ChR2-IO, blue). **e**, Population histogram of simple spike firing rate (SSpk, grey) and complex spike probability (CSpk, red) (n=74 trials, N=4 units from 2 animals). **f,g** As in d,e but for fiber placement in the cerebellar cortex, targeting CF terminals (CF-ChR2-Ctx, n=211 trials, N=15 cells from 5 animals). **h**, Spontaneous and laser-evoked SSpk and CSpk waveforms from an example Purkinje cell. **i**, Percentage of trials in which conditioned responses were observed (%CR) across daily training sessions of animals trained with a CF-ChR2-IO laser US (N=7 mice; thick line+shading: mean+/- s.e.m, thin lines: individual mice). Controls: wildtype mice (no ChR2 expression) with a fiber implanted in the IO presented with IO-laser US (N=2 mice). **j**, Average eyelid closure traces from CS-only trials of training sessions 2, 4 and 8 for the CF-ChR2-IO experiments shown in *j*. Shaded rectangle indicates where in the trial the US would have appeared. **k**, %CRs across training to a CF-ChR2-Ctx US (N=4 mice, plotted as in *j*). **l**, Average eyelid closure traces from CS-only trials of sessions 4, 6 and 8 for the CF-ChR2-Ctx experiments shown in *l* (N=4 mice). **m**, Average eyelid closures from CS-only trials after training to a CS+US interstimulus interval of 300ms (blue, N=4 mice), and 500ms (green, N=4 mice).
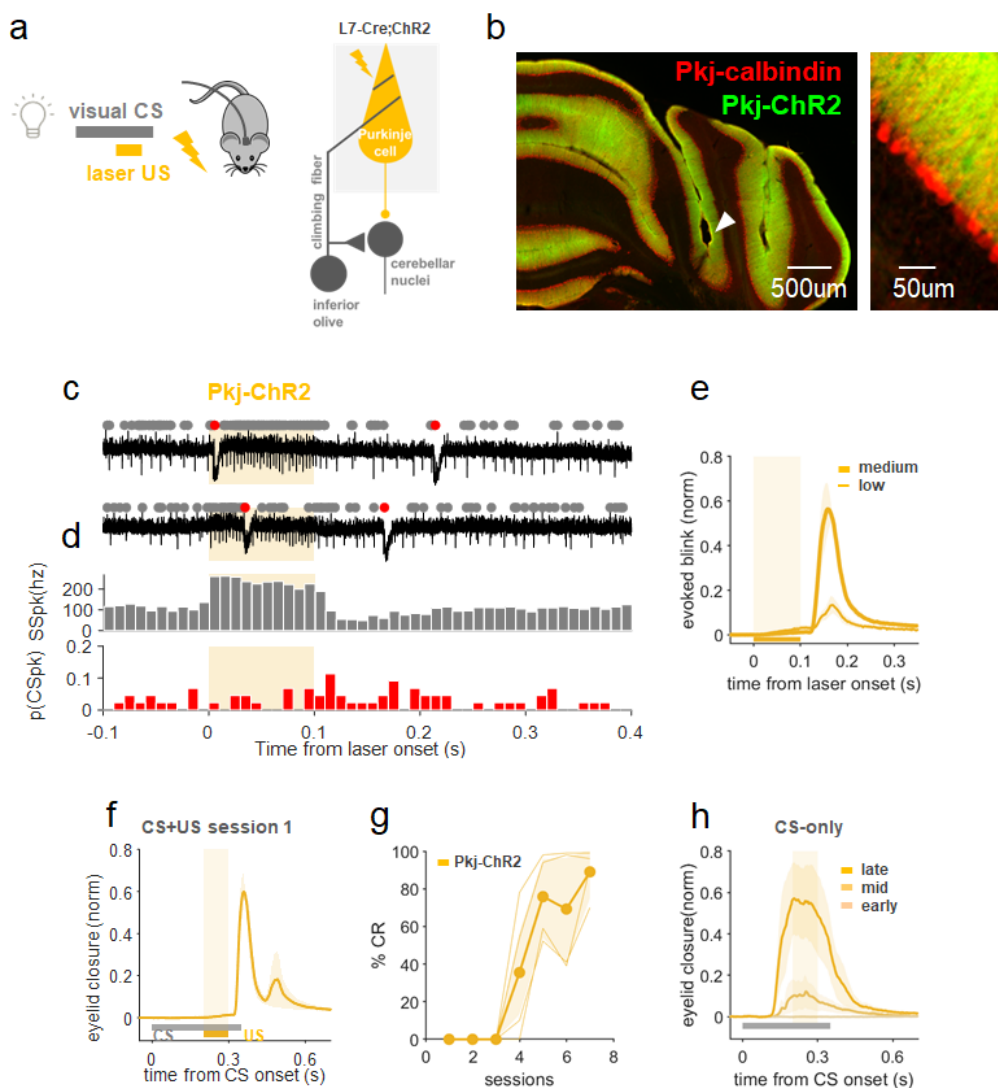
20

**Fig. 2. Optogenetic stimulation of Purkinje cells can substitute for a US to drive learning.**
**a**, Experimental scheme. L7-Cre;ChR2 mice were used to photostimulate Purkinje cells, which served as a US for conditioning. **b**, Example coronal section of cerebellar cortex indicating fiber placement in the eyelid area of the cerebellar cortex (white arrow) and labeling Purkinje cell ChR2 expression (green) and calbindin (red). **c**, Example electrophysiological traces of Purkinje cell simple spikes (grey dots) and complex spikes (red) in response to Pkj-ChR2 laser stimulation (orange shading). **d**, Population histogram of simple spike rate (grey) and complex spike probability (red; n=44 trials, N=2 units from 2 mice). **e**, Average eyelid closures evoked by low and medium-power Pkj-ChR2 stimulation (N=4 mice). Note the blink at stimulus offset. **f**, Average eyelid closures on CS+US trials in the first training session showing the blink evoked by Pkj-ChR2-US laser stimulation (N=4 mice). **g**, %CR across training sessions to a Pkj-ChR2-US (N=4 mice, plotted as in Fig. 1). **h**, Average eyelid traces from CS-only trials of sessions 2, 4, and 7 of the experiments in *g*.
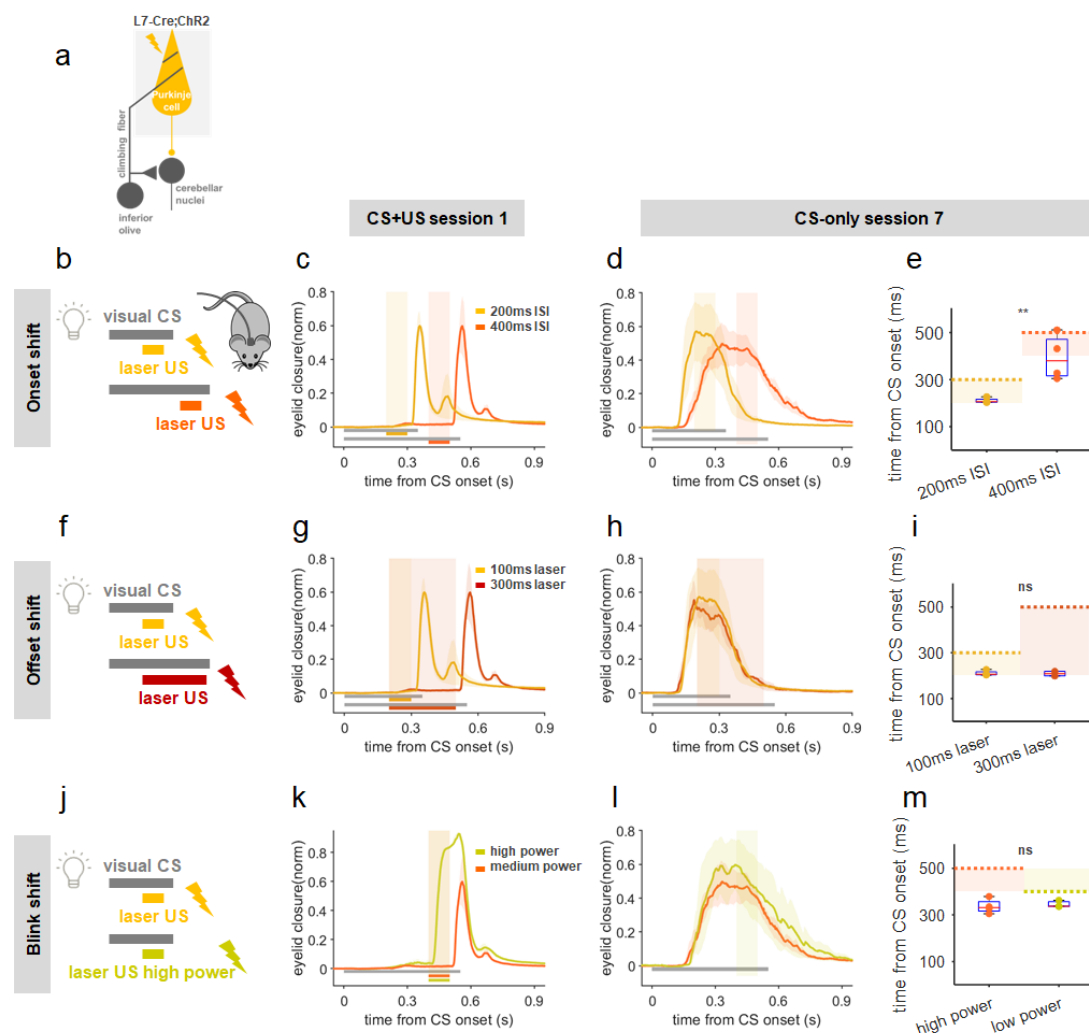
**Fig. 3. Learning evoked by optogenetic Purkinje cell stimulation is temporally coupled to stimulation onset, and not evoked blinks or simple spike modulation.**
**a,b,f,j**, Schemes for Pkj-ChR2-US experiments in which stimulation onset timing, duration, and intensity were varied systematically to dissociate candidate instructive signals (also see Supp. Fig. 2). **b**, US onset was shifted to obtain CS+US interstimulus intervals of 200 (yellow) or 400ms (orange). **c**, Evoked blinks on CS+US trials occurred at US offset in both conditions (N=4 mice each). **d**, Following training, the temporal profile of eyelid closures on CS-only trials depended on the timing of US-onset. **e**, The timing of peak eyelid closures on CS-only trials was later for the longer ISI (p=0.009**). Shaded rectangles indicate laser US duration and dashed lines indicate blink onset. Each dot is one mouse and box plots indicate 25th-75th percentiles with whiskers extending to most extreme data points. **f**, US duration was adjusted so that CS+US onset times were identical, but US offset (and blink) timing varied with respect to the CS. **g**, US-evoked blinks on CS+US trials occurred at stimulus offset (note the temporal correspondence with the blinks in *c*). Also see Supp. Fig. 2b-d. **h,i** the temporal profiles of CRs did not depend on the timing of stimulus offset or the evoked blink (p=0.87), but rather, stimulation onset. **j,k,** Laser intensity was adjusted to evoke a blink (associated with a decrease in simple spikes, see Supp. Fig. 2e-g) either at laser offset (orange, as above), or, with higher intensities, at laser onset (lime green; N=3 mice). Laser-US timings and durations were identical in the two conditions. **l,m** CR temporal profile depended only on the time of stimulation onset and did not vary with the timing of the evoked blink (p=0.67) or the direction of simple spike modulation (see Supp. Fig. 2e-h).
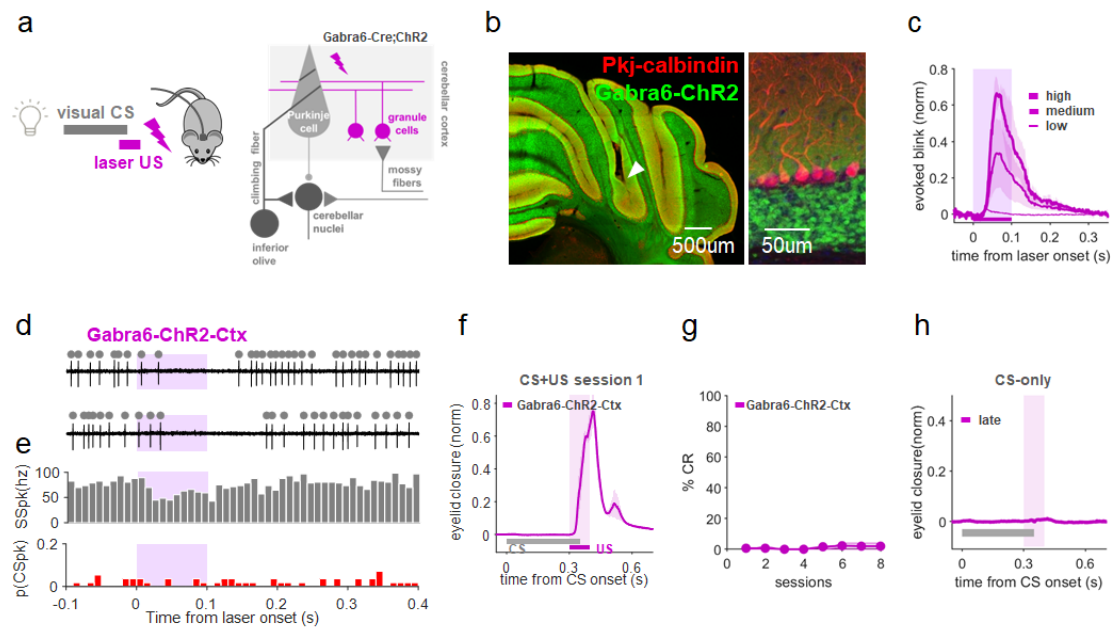
**Fig. 4. Optogenetic stimulation of cerebellar granule cells drives a blink but not learning.**
**a**, Experimental scheme. Gabra6-Cre;ChR2 mice were used to photostimulate cerebellar granule cells, which served as a US for conditioning. **b**, Example coronal sections of cerebellar cortex showing expression of ChR2 in granule cells (Gabra6-ChR2, green; Pkj-calbindin, red) and fiber placement in the eyeblink area of the cerebellar cortex (white arrow). **c**, Gabra6-ChR2 laser stimulation evoked intensity-dependent eyelid closures at stimulation onset (N=6 mice). **d**, Example electrophysiological traces of Purkinje cell simple spike (grey dots) and complex spike (red dots) modulation to Gabra6-ChR2 laser stimulation (purple shading). **e**, Population histograms (n=56 trials, N=3 cells from 2 animals). **f**, Average eyelid closures on CS+US trials of the first training session showing the blink evoked by Gabra6-ChR2 laser stimulation (purple, N=6 mice). **g**, %CR across sessions (N=6 mice). **h**, Average eyelid traces from CS-only trials of the last training session show no learning (purple, N=6 mice).
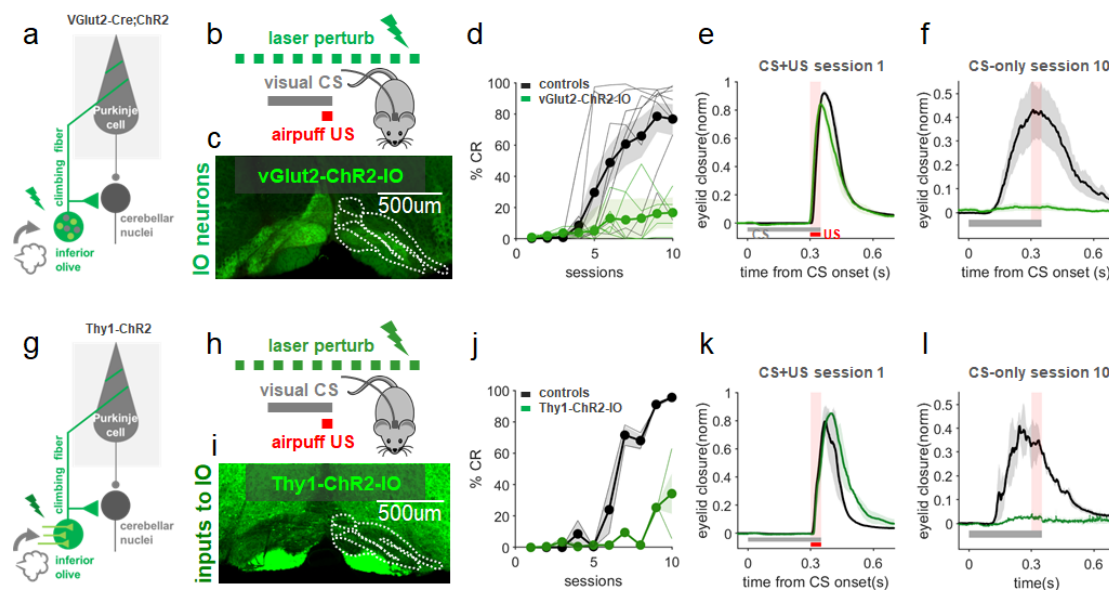
**Fig. 5. Perturbation of the inferior olive during CS+US trials impairs eyeblink conditioning.**
**a,b,g,h**, Experimental schemes for testing the effect of optogenetic IO perturbation on eyeblink conditioning to a sensory airpuff US. **a**, vGlut2-Cre;ChR2 mice were used to target ChR2 expression to excitatory neurons (see also Supp. Fig. 1). **b**, vGlut2-ChR2-IO laser perturbation (subthreshold to movement) began 1s before and ended 1s after each visual CS+airpuff-US trial. **c**, Coronal section showing ChR2 expression in the inferior olive. **d**, %CR across sessions with (green, N=5 mice) and without (black, N=8 mice) vGlut2-ChR2-IO laser perturbation. Littermate controls were with laser but no ChR2 expression (N=5) or vGlut-ChR2 with no laser (N=3). **e**, Blinks to an airpuff-US were intact during laser perturbation. **f**, Average eyelid closure traces from CS-only trials of the last training session reveal no learning in the perturbation condition. **g**, Thy1-ChR2 express ChR2 in excitatory inputs to the IO. **h-l**, Same as (*b-f*) but for Thy1-ChR2-IO perturbation (green, N=2 mice) and littermate controls (black, N=2 mice).
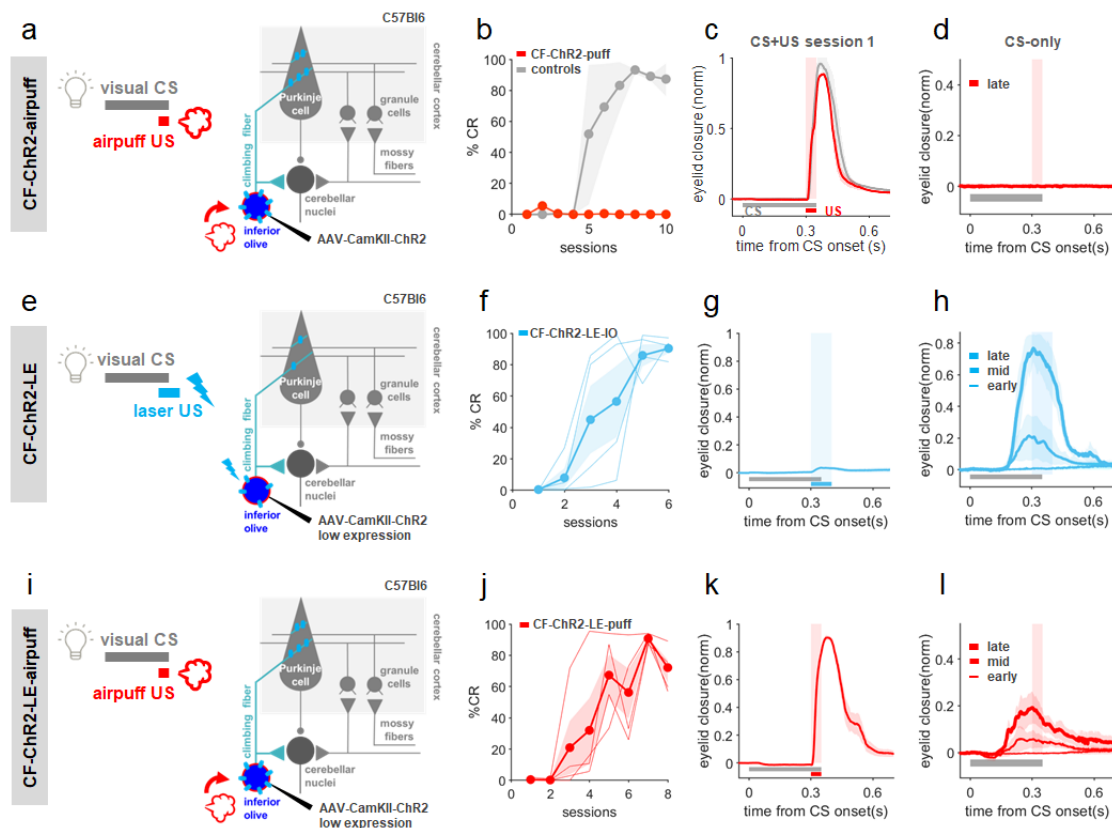
**Fig. 6. Moderate ChR2 expression in climbing fibers abolishes learning to a sensory US**
**a**, Experimental scheme. A visual CS was paired with a sensory airpuff-US in a traditional classical conditioning experiment in CF-ChR2 animals. **b**, CF-ChR2-puff animals, without any photostimulation, were unable to learn to an air-puff US (red, N=6 animals), while non-ChR2-expressing littermate controls (with an optic fiber implanted) learned well (grey, N=5 mice). **c**, both control mice (black; N=5) and animals expressing ChR2 in CFs but without any photostimulation (CF-ChR2-puff; red, N=6 mice) exhibited robust UR blinks on CS+US trials. **d**, Average eyelid traces from CS-only trials of the last training session reveal no learning in CF-ChR2-puff animals (red, N=6 mice). **e-i**, Conditioning with lower levels of ChR2 expression (CF-ChR2-LE). **e**, Experimental scheme for CF-ChR2-LE-IO experiments (Compare with Fig. 1i,j). An optogenetic US was paired with a visual CS in CF-ChR2-LE animals. **f**, %CR across training sessions (CF-ChR2-LE-IO, light blue, N=4 mice). **g**, CF-ChR2-LE-IO stimulation drives a small eye twitch on CS+US trials. **h**, Average eyelid traces from CS-only trials of sessions 1, 3, and 6 of the experiments in *f*. **i**, Experimental scheme for CF-ChR2-LE-puff experiments (Compare with panels a-d, above). A visual CS was paired with a sensory airpuff-US in a traditional classical conditioning experiment in CF-ChR2-LE animals. **j**, %CR across training sessions to an airpuff-US (CF-ChR2-LE-puff, red, N=4 mice). **k**, CF-ChR2-LE animals exhibited robust blinks on CS+US trials. **h**, Average eyelid traces from CS-only trials of sessions 2, 4, and 8 of the experiments in *j*.
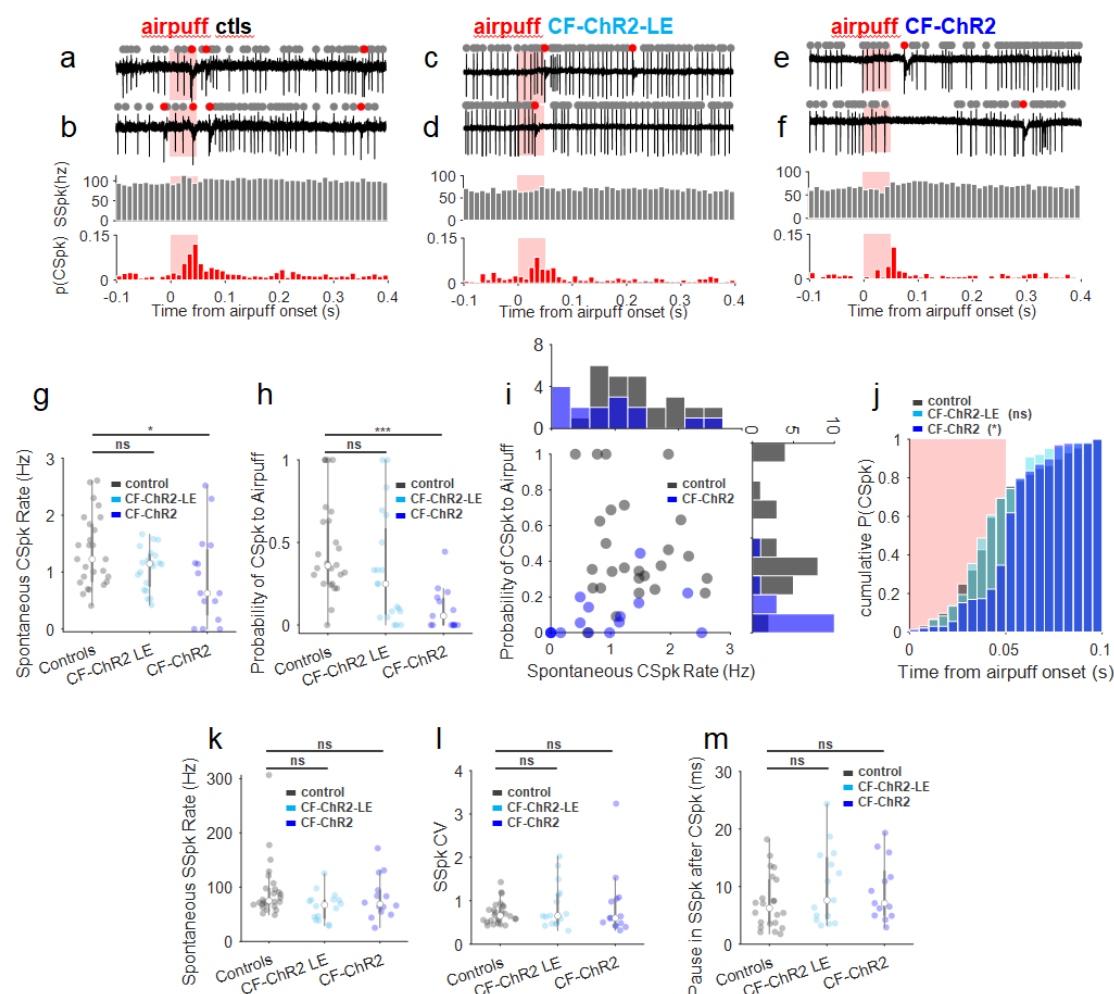
**Fig. 7. ChR2 expression is associated with subtle reductions in climbing fiber signaling that block learning**

**a,b**, Example electrophysiological traces and population histograms (N=26 units from 4 mice) of Purkinje cell simple spikes (grey) and complex spikes (red) from control mice in response to an airpuff to the eye. **c,d**, Example electrophysiological traces and population histograms from mice expressing low levels of ChR2 in CFs (CF-ChR2-LE; N=20 units from 4 mice). **e,f**, Example electrophysiological traces and population histograms from CF-ChR2 mice (standard expression levels; N=15 units from 5 mice). **g**, Spontaneous CSpk firing rate for each Purkinje cell recorded from control (black), CF-ChR2-LE (light blue) and CF-ChR2 (blue) mice (CF-ChR2 vs ctls p=0.04*; CF-ChR2-LE vs ctls p=0.07ns). **h**, Probability of an airpuff-evoked complex spike for each Purkinje cell recorded (control vs. CF-ChR2 p=0.00003***; control vs. CF-ChR2-LE p=0.16ns). **i**, p(CSpk) to airpuff as a function of spontaneous CSpk rate for each Purkinje cell. **j**, Normalized cumulative histogram of the timing of the first CSpk after airpuff onset, (grey: controls N=26 cells from 4 animals; light blue, CF-ChR2-LE, N=20 cells from 4 animals; dark blue: CF-ChR2 N=15 cells from 5 mice). Shaded rectangle indicates time of airpuff. KS-test CF-ChR2 vs ctls, p=0.03* and CF-ChR2-LE vs ctls, p=0.67n.s. **k-m**, Simple spike statistics for each Purkinje cell recorded from control (black), CF-ChR2-LE (light blue) and CF-ChR2 (blue) mice. **k**, Spontaneous firing rate (CF-ChR2 vs ctls p=0.41ns; CF-ChR2-LE vs ctls p=0.05ns). **l**, Coefficient of variation (CF-ChR2 vs ctls p=0.33ns; CF-ChR2-LE vs ctls p=0.19ns). **m**, Average pause in SSpk activity after a CSpk (CF-ChR2-LE vs ctls p=0.24 ns; CF-ChR2 vs ctls p= 0.15 ns).

## SUPPLEMENTAL FIGURES
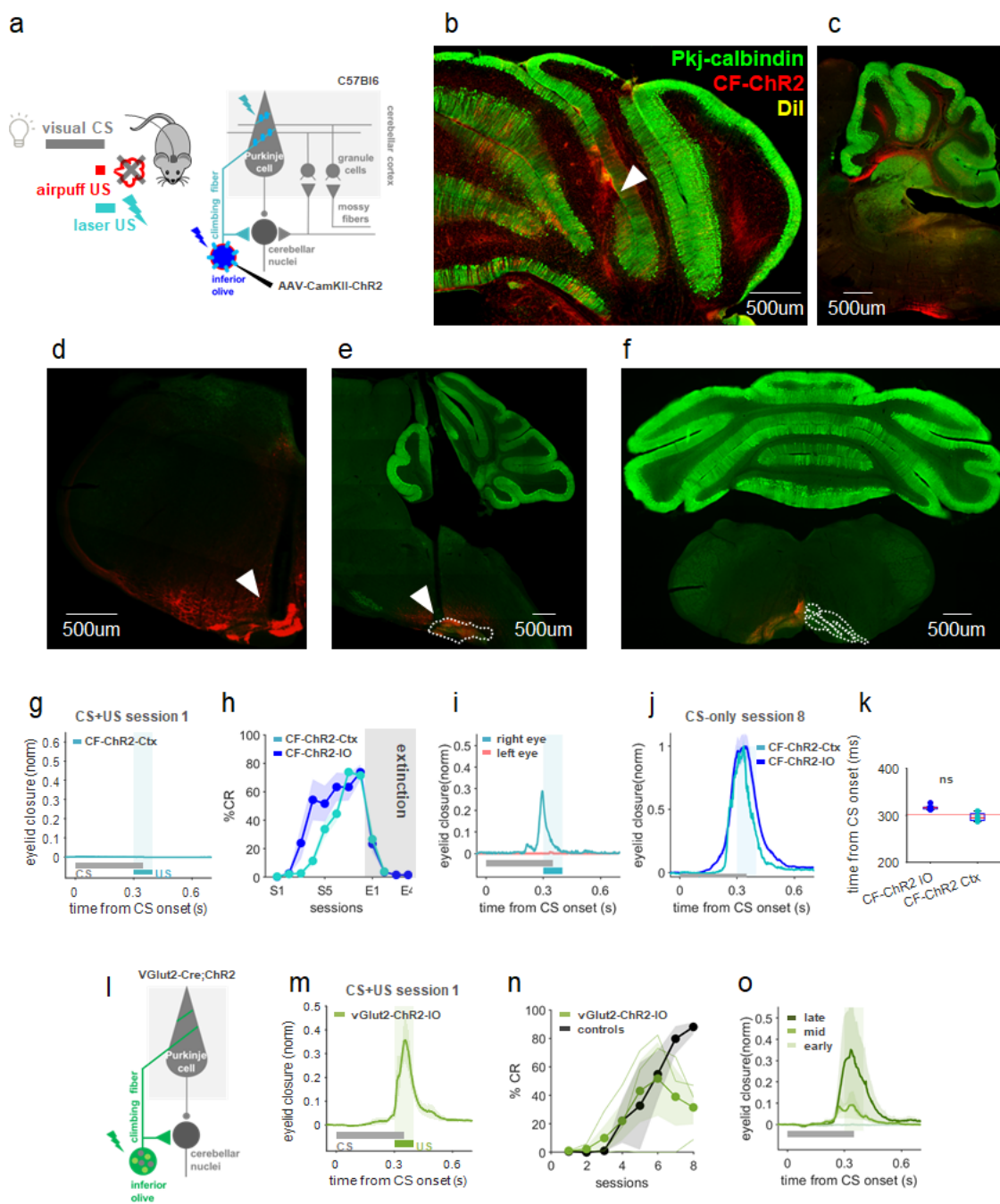


**Supp. Fig. 1. Multiple genetic and anatomical strategies for targeting IO neurons**
**a**, Experimental scheme. **b**, Example coronal section showing fiber placement (white arrow), at the eyelid area of the right cerebellar cortex of CF-ChR2 animals. **c**, Example sagittal section showing ChR2 expression in climbing fiber projections to the cerebellar cortex. **d**, Example coronal section showing CF-ChR2 expression and optical fiber placement (white arrow) at the left IO. **e**, Example sagittal section showing CF-ChR2 expression and fiber placement (white arrow) at the left IO. **f**, Example coronal section showing ChR2 expression at the left inferior olive of CF-ChR2 expressing animals. **g**, Average eyelid closure trace from CS+US trials of the first training session showing no reflexive eyeblink to CF-ChR2-Ctx laser stimulation (N=4 mice). **h**, Average percentage of conditioned response (%CR) over the course of multiple training (S1-S8) and extinction sessions (E1-E4, where only the visual CS is presented without a US) of animals with CF-ChR2 laser stimulation at the cerebellar cortex or at the inferior olive as US (CF-ChR2-Ctx in cyan, N=4 mice; CF-ChR2-IO in blue, N=3 mice). **i**, Average eyeblink

27

closure traces after eyeblink learning with CF-ChR2 laser stimulation at the cerebellar cortex as an US. Conditioning was unilateral (right eye in cyan, left eye in red; N=2 mice). **j,** Normalized traces illustrate broader CR timing for the CF-ChR2-IO condition (for the experiments shown in *h*). **k**, Timing of peak eyelid closures are subtly later for the CF-ChR2-IO condition, across mice (316ms vs. 294ms for CF-ChR2-Ctx; p=0.2ns). Each dot is one mouse and box plots indicate 25th-75th percentiles with whiskers extending to most extreme data point. **l**, Experimental scheme for experiments stimulating glutamatergic IO neurons as a US (vGlut2-ChR2-IO; Supp. Table 1). **m,** Average eyelid closures on CS+US trials in the first training session showing the blink evoked by vGlut2-ChR2-IO-US laser stimulation (N=3 mice). **n**, %CR across sessions for learning to a vGlut2-ChR2-IO-US (green, N=3 mice) and controls (expressing ChR2 but without laser stimulation, learning to an airpuff US). **o**, Average eyelid closure traces from CS-only trials of S2, S4 and S8 training sessions for a vGlut2-ChR2-IO-US (N=3).
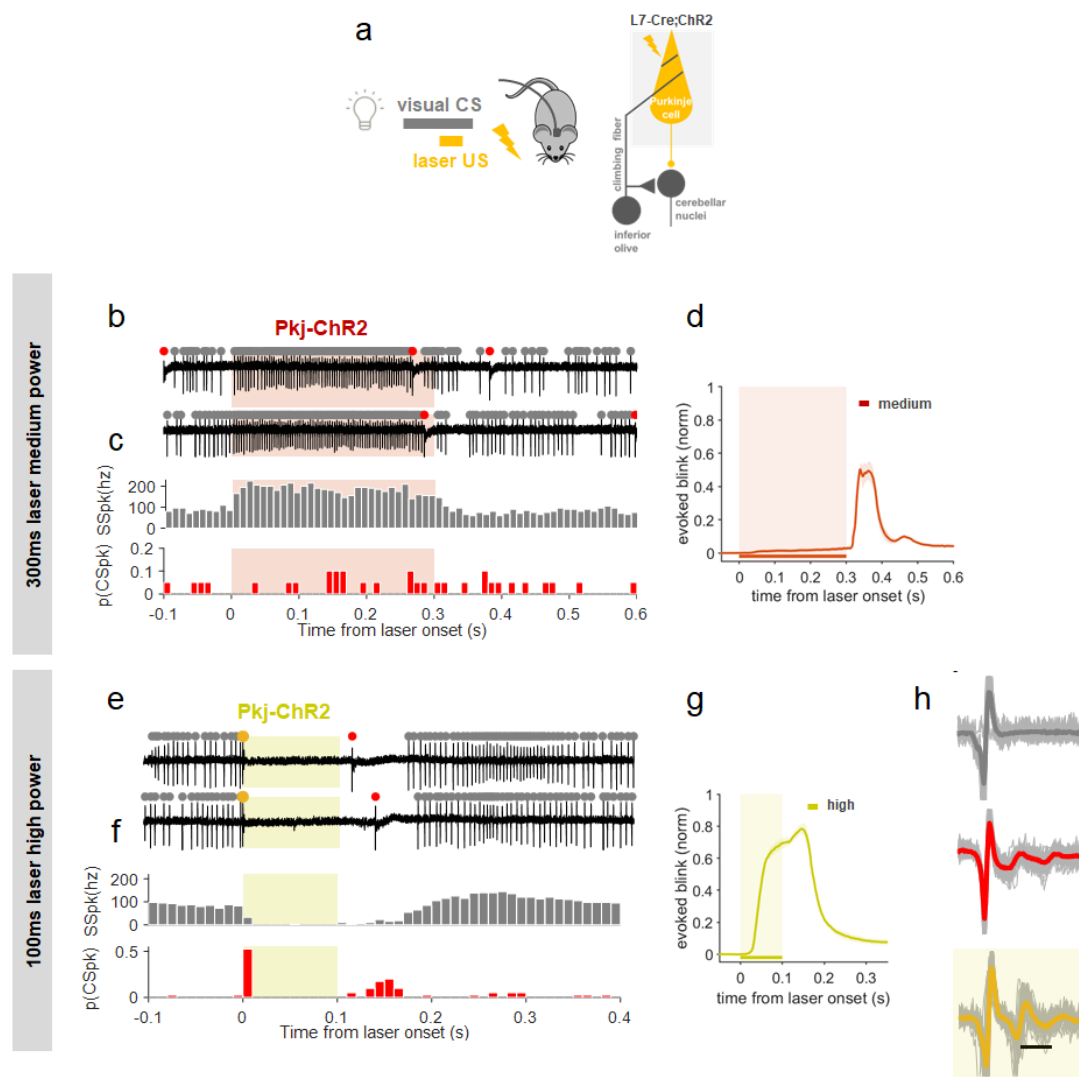
**Supp. Fig. 2. Varying intensity and duration of Purkinje cell optogenetic stimulation to dissociate stimulation onset, simple spike modulation, and evoked blinks**

**a**, Experimental scheme for pairing a visual CS with optogenetic Purkinje cell-US. **b,** Example electrophysiological traces from a Purkinje cell with identified simple spikes (grey dots) and complex spikes (red dots) in response to 300ms medium intensity Pkj-ChR2 laser stimulation at the cerebellar cortex (Pkj-ChR2-Ctx-med). (Corresponds to Fig. 3f-i.) **c**, Population histogram of simple spike rates (SSpk, grey) and complex spike probabilities (CSpk, red)(N=1 unit from 1 mouse). **d**, Average eyelid closures to 300ms Pkj-ChR2-Ctx medium intensity laser stimulation (N=2 mice, shading represents time of laser stimulation). **e-h** Higher intensity Pkj-ChR2-Ctx laser stimulation was used to evoke a pause in simple spikes and a short-latency evoked blink at stimulus *onset.* (Corresponds to Fig. 3j-m) **e,f,** Simple and complex spike traces and histograms (N=2 units from 2 mice). **g**, Pkj-ChR2 laser stimulation at higher intensities yields a blink at stimulus *onset* (N=3 mice, shading represents laser stimulation). **h,** simple spike (grey) and spontaneous complex spike (red) waveforms. Yellow trace represents complex spike-like events at stimulus onset. Note the correspondence to spontaneous complex spike waveforms (red).
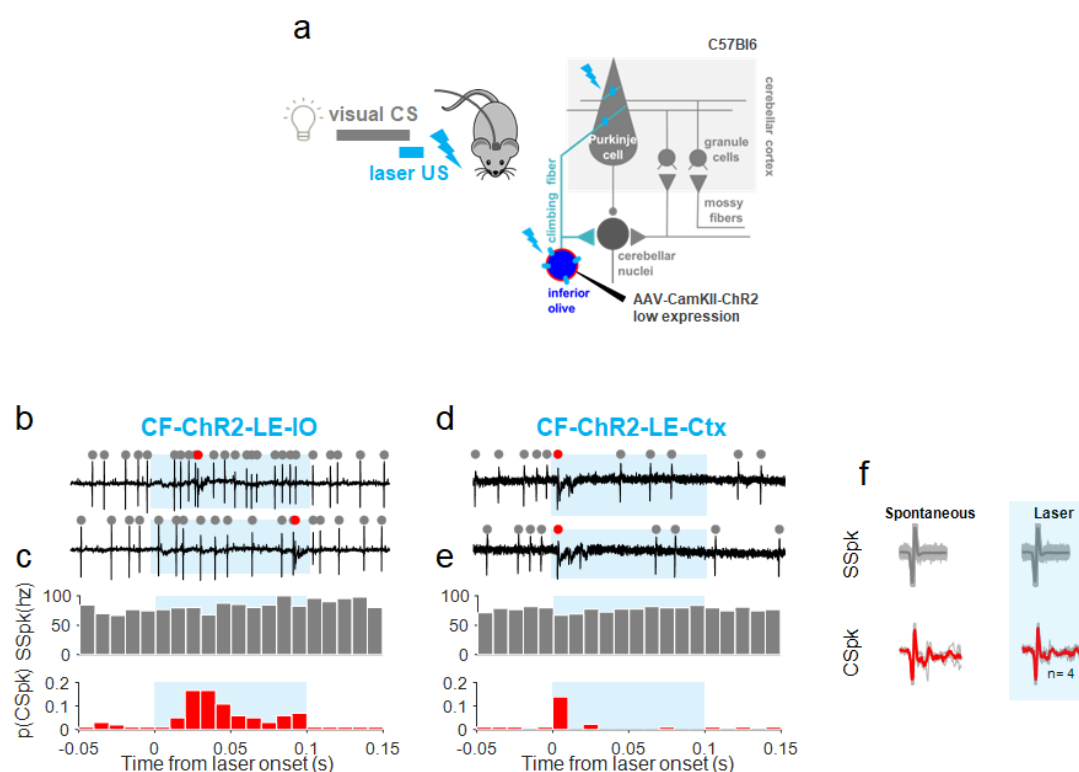
**Supp. Fig. 3. Optogenetically-evoked Purkinje cell complex spikes with lower CF-ChR2 expression**

**a**, Experimental scheme for CF-ChR2-low expression experiments (CF-ChR2-LE). **b,c,** Example electrophysiological traces from a Purkinje cell showing simple spikes (grey) and complex spikes (red) in response to laser stimulation at the IO (CF-ChR2-LE-IO). **c**, Population histogram (n=102 trials, N=8 cells from 2 mice). **d,e** Example traces and population histograms for CF-ChR2-LE stimulation in the cerebellar cortex (CF-ChR2-LE-Ctx; n=94 trials, N=10 cells from 2 mice). **f**, Spontaneous and laser-evoked SSpk and CSpk waveforms from an example Purkinje cell.

| Fig # | Candidate instructive signal | US modality | Perturbation | Learning result | UR (blink) to US? | CSpk+ model predict learning? | SS- model predict learning? | congruence UR <-> learning (Could the blink itself as an instructive signal explain learning?) | congruence SS(-) <-> learning (Could decreases in SS rate as an instructive signal explain learning?) | congruence CSpk <-> learning (Could CSpks as an instructive signal explain learning?) |
|---|---|---|---|---|---|---|---|---|---|---|
| | control conditions | airpuff | none | yes | yes | yes | yes | yes | yes | yes |
| 1 | CF-ChR2-Ctx | opto | optostim (CSpk+) | yes | no | yes | | no | | yes |
| 1 | CF-ChR2-IO | opto | optostim (CSpk+) | yes | no | yes | | no | | yes |
| 2, 3 | Pkj-ChR2-med (onset) | opto | optostim-onset (SS+) | yes | no | yes* | no | no | no | yes* (with CSpk-like event at optostim onset) |
| 3, Supp. 2 | Pkj-ChR2-med (offset) | opto | optostim-offset (SS-) | no | yes | no | yes | no | no | yes |
| 3, Supp. 2 | Pkj-ChR2-high | opto | optostim-onset (SS-) | yes | yes | yes | yes | yes | yes | yes (via CSpk-like event at optostim onset) |
| 4 | Gabra6-ChR2-Ctx | opto | optostim-onset (SS-) | no | yes | no | yes | no | no | yes |
| Supp. 1 | vGlut2-ChR2-IO | opto | optostim (CSpk+) | yes | yes | yes | | yes | | yes |
| 5 | vGlut2-ChR2-IO | airpuff | perturb-IO | no | yes | no | | no | | yes |
| 5 | Thy1-ChR2-IO | airpuff | perturb-IO | no | yes | no | | no | | yes |
| 6, 7 | CF-ChR2-puff | airpuff | expression (CSpk-) | no | yes | no | yes | no | no | yes |
| 6, Supp. 3 | CF-ChR2-LE | opto | optostim (CSpk+) | yes | yes | yes | | yes | | yes |
| 6, 7 | CF-ChR2-LE-puff | airpuff | none (low expression) | yes | yes | yes | | yes | | yes |

**Supp. Fig. 4. Summary of candidate instructive signals tested in the study and explanatory power of three models for cerebellar learning**

**a**, Cerebellar circuit for eyeblink conditioning, highlighting the different strategies used in the study. **b**, Summary table indicating the candidate instructive signal evaluated with each experiment, ordered and color-coded by Figure number. For each candidate tested, the presence/ absence of robust learning is indicated, together with the predictions of blink-, CSpk-, or SS-related models for learning. The last 3 columns assess the congruence between each model's prediction and the learning result that was observed.